

# Gradient-based Sparse Principal Component Analysis with Extensions to Online Learning

Yixuan Qiu, Jing Lei, and Kathryn Roeder

Department of Statistics and Data Science, Carnegie Mellon University  
Pittsburgh, PA 15213, {yixuanq, jinglei, roeder}@andrew.cmu.edu

**Abstract:** Sparse principal component analysis (PCA) is an important technique for dimensionality reduction of high-dimensional data. However, most existing sparse PCA algorithms are based on non-convex optimization, which provide little guarantee on the global convergence. Sparse PCA algorithms based on a convex formulation, for example the Fantope projection and selection (FPS), overcome this difficulty, but are computationally expensive. In this work we study sparse PCA based on the convex FPS formulation, and propose a new algorithm that is computationally efficient and applicable to large and high-dimensional data sets. Nonasymptotic and explicit bounds are derived for both the optimization error and the statistical accuracy, which can be used for testing and inference problems. We also extend our algorithm to online learning problems, where data are obtained in a streaming fashion. The proposed algorithm is applied to high-dimensional gene expression data for the detection of functional gene groups.

**Keywords:** sparse principal component analysis, dimensionality reduction, convex optimization, gradient method, online learning.

## 1 Introduction

Principal component analysis (PCA, [Pearson, 1901](#); [Hotelling, 1933](#)) is a classical yet indispensable dimensionality reduction technique in statistics and machine learning. PCA generates higher-level features of the raw data by computing uncorrelated linear combinations of the original variables that retain the maximum amount of variation of the raw data. Moreover, PCA can process data sets that have a variable dimension

larger than the sample size. Such desirable properties of PCA make it one of the most popular preprocessing techniques in multivariate statistics.

In the high-dimensional setting where the number of variables can be comparable to or larger than the sample size, PCA suffers from the well-known curse-of-dimensionality. For instance, [Johnstone and Lu \(2009\)](#) and [Jung and Marron \(2009\)](#) showed that when the number of variables is much larger than the sample size, PCA can behave poorly in estimating the principal components (PCs), even with a simple population covariance structure, producing misleading results in scenarios that it was exactly invented for.

On the other hand, these theoretical works also motivated the development of a variant of PCA, the sparse PCA method, which overcame many of the limitations of traditional PCA in high-dimensional settings. Sparse PCA works similarly to the original PCA, but requires the PCs to be sparse. Here sparsity means that the linear combination involves only a small number of variables. Such a sparsity requirement greatly reduces the number of coefficients to estimate, and enhances the interpretability of the estimated PCs. Pioneer works on sparse PCA include [Jolliffe et al. \(2003\)](#); [Johnstone and Lu \(2009\)](#); [Zou et al. \(2006\)](#) etc.. Since then sparse PCA has found wide applications in keyword extraction for text data ([Zhang and Ghaoui, 2011](#)), fault detection for industrial processes ([Grbovic et al., 2012](#); [Gajjar et al., 2018](#)), genomics and genetics ([Lee et al., 2012](#); [Zhu et al., 2017](#)), among many others.

One major challenge of sparse PCA is the computation. Unlike ordinary PCA, which can be efficiently solved using well-studied eigen decomposition methods such as the power method, the original formulation of sparse PCA ([Jolliffe et al., 2003](#)) involves solving a sparsity constrained eigenvalue problem that is computationally hard. Existing fast algorithms for nonconvex objective functions ([Zou et al., 2006](#); [Witten et al., 2009](#); [Journée et al., 2010](#)) generally do not guarantee the global convergence and rely on the initial values. This limitation has an adverse impact on the applications of sparse PCA, especially in rigorous statistical inference and scientific research. Alternatively, [d'Aspremont et al. \(2005\)](#); [Vu et al. \(2013\)](#) proposed convex formulations of the sparse PCA problem using semidefinite programming, which are computationally expensive for large matrices commonly seen in modern applications such as text mining and bioinformatics. Therefore, a sparse PCA algorithm that has both a global convergence guarantee and an efficient implementation is in great need.

The computational difficulties of the existing sparse PCA algorithms also limit their applications in an important area: the online learning methods that arise from the demand to analyze large-scale streaming data. As the volumes of data sets are rapidly

growing and data collection procedures become more dynamic, it is challenging to store and analyze all the observations at the same time, so it is preferable to build and update models immediately after a new data point is obtained. Online PCA algorithms have been extensively studied in the literature (Oja and Karhunen, 1985; Warmuth and Kuzmin, 2008; Marinov et al., 2018; Li et al., 2018), but the work on online sparse PCA is scarce (Yang and Xu, 2015; Wang and Lu, 2016). The difficulty of online sparse PCA mainly comes from the fact that existing methods could not express sparse PCA as an easy-to-solve optimization problem. A statistically and computationally provable online sparse PCA algorithm remains an open problem.

To overcome the challenges above, in this article we propose new computational algorithms for sparse PCA and its online versions. The main contributions of our work are as follows. First, by analyzing the geometry of sparse PCA, we represent its solution by an *unconstrained* convex optimization problem. As a result, efficient gradient-based and projection-free algorithms are developed, whose output can be used as good initial values for nonconvex methods. Second, the unconstrained convex formulation is extended to the online setting, and two different online sparse PCA algorithms are proposed, depending on whether the data sets have large sample sizes or high dimensions. To our best knowledge, these are the first online sparse PCA algorithms that can be computed efficiently and have global convergence guarantees for a general covariance model. Third, for each algorithm, both the optimization error and the statistical accuracy are rigorously analyzed with nonasymptotic and explicit bounds.

The theoretical justifications are supported by various simulation experiments. For the batch version of sparse PCA, we demonstrate that our new algorithm has much faster convergence than the existing method given the same computational time. In online settings, the proposed methods also have convergence results that are consistent with the theory. Moreover, we apply the new sparse PCA algorithm to a real high-dimensional gene expression data set and successfully detect differential co-expression patterns in schizophrenia subjects compared to a control group. Proofs of theorems are given in the supplementary material.

## 2 Overview of Sparse PCA

From a statistical point of view, the major target of PCA is to estimate the factor loadings of each PC from the noisy data. Suppose the data set is a sample of independent and identically distributed random vectors  $Z_1, \dots, Z_n \in \mathbb{R}^p$  with zero means and the

true covariance matrix  $\Sigma = \text{Cov}(Z_i)$ . Let  $\theta_i = \theta_i(A), i = 1, \dots, p$  represent the ordered eigenvalues of a matrix  $A$ ,  $\theta_1 \geq \dots \geq \theta_p$ , and  $\gamma_i(A)$  be the associated eigenvector. Then PCA aims at estimating the  $p \times d$  matrix  $\Gamma = (\gamma_1(\Sigma), \dots, \gamma_d(\Sigma))$  containing the top  $d$  eigenvectors of  $\Sigma$ , which is typically referred to as the factor loading matrix.

The ordinary PCA estimates  $\Gamma$  by first computing the sample covariance matrix,  $S = n^{-1} \sum_{i=1}^n Z_i Z_i^T$ , and then extracting the leading  $d$  eigenvectors of  $S$ . However, it has been well studied that in the high-dimensional case  $p \gg n$ ,  $S$  can be a poor estimator for  $\Sigma$ , so the ordinary PCA method is also likely to fail. To enable PCA in high-dimensional data, one needs to make stronger assumptions on the data distribution. For example, in sparse PCA,  $\Gamma$  is assumed to contain many zero entries, so that the number of unknown coefficients are greatly reduced. This idea leads to the following core assumption throughout this article.

**Assumption 1.** *The factor loading matrix  $\Gamma$  has at most  $s$  nonzero rows, and the  $d$ -th eigengap of  $\Sigma$  is nonzero,  $\delta_d = \theta_d(\Sigma) - \theta_{d+1}(\Sigma) > 0$ .*

Such a sparsity assumption has been considered as the ‘‘row sparsity’’ in [Vu and Lei \(2013\)](#), which assumes that the leading  $d$ -dimensional principal subspace is unique and is supported on a small number of coordinates. This is a quite strong assumption, but in many applications such as genetics, a sparse factor loading vector is often preferred due to the better interpretability. Assumption 1 is made to facilitate the mathematical investigation of sparse PCA algorithms.

Under the sparsity assumption, sparse PCA has been formulated in many different ways, including the lasso approach in PCA ([Jolliffe et al., 2003](#)), regression-based formulation ([Zou et al., 2006](#)), iterative thresholding methods ([Shen and Huang, 2008](#); [Witten et al., 2009](#); [Ma, 2013](#); [She, 2017](#)), the generalized power method ([Journée et al., 2010](#)), among many others. Also see [Zou and Xue \(2018\)](#) for a recent review of various sparse PCA methods. Despite the rich literature, most of the existing algorithms suffer from two common issues. The first issue is from the perspective of optimization. The majority of the existing sparse PCA algorithms are formulated as nonconvex optimization problems, which possess some local convergence properties at best. Therefore, such algorithms highly rely on the initial values, which are typically unavailable *a priori*. The second issue is on the statistical aspect. To recover the true population eigenvectors, sparse PCA methods typically impose some additional structural assumptions on the covariance matrix, for instance the spiked covariance model.

In comparison, convex optimization has the advantage of superior convergence prop-

erties. In most cases, a proper algorithm can iteratively find the global optimum irrespective of the initial values. Such a property makes convex optimization extremely popular in statistical and machine learning models. For sparse PCA, [d’Aspremont et al. \(2005\)](#) proposed a formulation called DSPCA that takes the form of a convex semidefinite program. Let  $\|A\|_{p,q} = \{\sum_{j=1}^n (\sum_{i=1}^m |a_{ij}|^p)^{q/p}\}^{1/q}$  denote the  $L_{p,q}$  norm for an  $m \times n$  matrix  $A$ , and then DSPCA finds an estimator for the projection matrix  $\Pi_1 = \gamma_1 \gamma_1^T$  using the solution to the following optimization problem:

$$\begin{aligned} \max \quad & \text{tr}(SX) \\ \text{s.t.} \quad & \text{tr}(X) = 1, \quad \|X\|_{1,1} \leq s_1, \quad \text{and } O \preceq X, \end{aligned} \tag{1}$$

where  $s_1$  is a parameter to control the sparsity of the solution,  $O$  is the zero matrix, and  $A \preceq B$  means  $B - A$  is nonnegative definite.

Since DSPCA only extracts the first component, [Vu et al. \(2013\)](#) developed a generalized model, called Fantope projection and selection (FPS), to estimate the top- $d$  projection matrix  $\Pi = \Gamma \Gamma^T$ . The optimization problem of FPS is given by

$$\begin{aligned} \max \quad & \text{tr}(SX) - \lambda \|X\|_{1,1} \\ \text{s.t.} \quad & O \preceq X \preceq I \text{ and } \text{tr}(X) = d, \end{aligned} \tag{2}$$

where  $\lambda$  is the sparsity penalty parameter. The convex constraint set  $\mathcal{F}^d = \{X : O \preceq X \preceq I \text{ and } \text{tr}(X) = d\}$  is called the Fantope. When  $d = 1$ , FPS becomes equivalent to DSPCA. The FPS formulation has attractive statistical properties ([Vu et al., 2013](#); [Lei and Vu, 2015](#)), and can be solved in polynomial time using the alternating direction method of multipliers (ADMM, [Boyd et al., 2011](#)), an iterative algorithm for constrained convex optimization problems.

However, the existing ADMM-based FPS algorithm is shown to be slow, since each iteration of the algorithm requires projecting a  $p \times p$  matrix onto the Fantope, which involves a full eigen decomposition of the  $p \times p$  matrix. When the dimensionality of  $S$  is high, for example in genetic studies, the computational cost of the ADMM algorithm is  $\mathcal{O}(p^3)$  per iteration. As a consequence, the applicability of FPS is substantially limited by the cubic growth of computing time per iteration, and a more computationally efficient FPS algorithm is much desired.

## 3 A New Projection-Free Algorithm for Sparse PCA

### 3.1 Gradient-based Methods for Large-scale Optimization

In convex optimization problems, if the objective function is twice differentiable, then the standard approach is the Newton–Raphson iteration based on the Hessian matrix. However, when the parameter dimension is too high so that the Hessian matrix is too large, or when the objective function is not differentiable, one often needs to resort to the first-order methods that rely only on the gradient or subgradient of the objective function. In this article we refer to such methods as the gradient-based methods.

The gradient-based methods have successful applications in many statistical and machine learning problems, but their computational efficiency heavily depends on the form of the optimization problem. Take the FPS problem (2) as an example, which has two difficulties to deal with. First, the objective function is nonsmooth, and second, the solution is sought within a constrained set  $\mathcal{F}^d$ . If one ignores the nonsmoothness, then a simple gradient-based method is the projected subgradient descent algorithm,

$$X_{k+1} = \mathcal{P}_{\mathcal{F}^d}(X_k + \alpha_k S - \alpha_k \lambda \cdot \text{sign}(X)), \quad (3)$$

where  $\alpha_k$  is the step size at iteration  $k$ , and the symbol  $\mathcal{P}_C(x) = \arg \min_{y \in C} \|y - x\|$  means the projection of  $x$  onto a convex set  $C$ , with  $\|\cdot\|$  being the Euclidean norm. In (3), the sign function  $\text{sign}(X)$  is the subgradient of the nonsmooth  $\|X\|_{1,1}$  term. To overcome the nonsmoothness, a faster optimization scheme is given by the ADMM algorithm using proximal operators, where the proximal operator of a convex function  $f$  with step size  $\alpha$  is defined as  $\mathbf{prox}_{\alpha f}(x) = \arg \min_u \{f(u) + (2\alpha)^{-1} \|u - x\|^2\}$ , and can be seen as a special gradient. Let  $\mathcal{S}_\alpha(x) = \text{sign}(x) \cdot \max\{|x| - \alpha, 0\}$  be the soft-thresholding operator, and  $\mathcal{S}_\alpha(X) = \mathbf{prox}_{\alpha \|\cdot\|_{1,1}}(X)$  means applying  $\mathcal{S}_\alpha(x)$  to the matrix  $X$  elementwisely. Then the ADMM algorithm proceeds as follows (Vu et al., 2013),

$$\begin{aligned} X_{k+1} &= \mathcal{P}_{\mathcal{F}^d}(Y_k - U_k + \alpha S), \\ Y_{k+1} &= \mathcal{S}_{\alpha\lambda}(X_{k+1} + U_k), \quad U_{k+1} = U_k + X_{k+1} - Y_{k+1}, \end{aligned} \quad (4)$$

where  $Y$  and  $U$  are auxiliary variables, and  $\alpha$  is the step size.

For both (3) and (4), however, the projection operator  $\mathcal{P}_{\mathcal{F}^d}$  is unavoidable, which becomes the major bottleneck of the overall algorithms. Therefore, to accelerate the convex sparse PCA, it is necessary to reformulate the objective function and get rid of the time-consuming projection operator.

### 3.2 Projection-free Optimization on Intersection of Convex Sets

The massive cost of  $\mathcal{P}_{\mathcal{F}^d}$  stems from the complexity of the constraint set  $\mathcal{F}^d$ , which is the intersection of three convex sets:  $\mathcal{F}_1 = \{X : \text{tr}(X) = d\}$ ,  $\mathcal{F}_2 = \{X : X \succeq O\}$ , and  $\mathcal{F}_3 = \{X : X \preceq I\}$ . Each one of the three sets has a simple structure. However, when taking the intersection, the associated projection operator becomes the major obstacle for an efficient algorithm.

To this end, in this section we first develop a general scheme for solving optimization problems on the intersection of convex sets. We show that under certain assumptions, the complex constraint can be recast as a penalty term added to the objective function, so that the original constrained optimization problem is equivalent to an unconstrained one. Moreover, under a proper setting, the new problem can bypass the complicated operators on the intersection set, and directly work on each individual convex set, which significantly reduces the computational difficulty.

The optimization problem considered in this section has the following form:

$$\min_{x \in \mathcal{K}} f(x), \quad \mathcal{K} = C_1 \cap \cdots \cap C_l \cap G_1 \cap \cdots \cap G_m, \quad (5)$$

where  $f(x)$  is a convex function,  $C_i$ 's are closed convex sets, and  $G_i$  is defined by  $G_i = \{x : g_i(x) \leq 0\}$ . Each constraint function  $g_i(x)$  is a convex function, and  $\mathcal{K}$  is contained in a closed convex set  $\mathcal{X} \subset \mathbb{R}^p$  whose projection operator  $\mathcal{P}_{\mathcal{X}}$  is trivial. The intersection set  $\mathcal{K}$  is decomposed in such a way that the projection operators  $\mathcal{P}_{C_i}$  and the constraint functions  $g_i(x)$  are easy to compute.

The problem with  $m = 0$  has been studied in the literature (Kundu et al., 2018), but it is not useful for the FPS problem since  $\mathcal{P}_{\mathcal{F}_2}$  and  $\mathcal{P}_{\mathcal{F}_3}$  are still expensive. As will be shown in the next section, the inclusion of the  $G_i$  sets overcomes this difficulty, since the constraint functions only involve the extreme eigenvalues of  $X$ . The problem with  $l = 0$  and  $m = 1$  has been studied in Mahdavi et al. (2012) and Yang et al. (2017). Obviously, our formulation in (5) is a generalization to the ones mentioned above. We then make the following assumptions on the objects involved in (5).

**Assumption 2.**  $f(x)$  is Lipschitz continuous on  $\mathcal{X}$  with the Lipschitz constant  $L > 0$ :  $|f(x) - f(y)| \leq L\|x - y\|$ ,  $\forall x, y \in \mathcal{X}$ .

**Assumption 3.** For  $i = 1, \dots, m$ , (a)  $x \in \mathcal{X}$  implies  $\mathcal{P}_{G_i}(x) \in \mathcal{X}$ ; (b) there exists a constant  $\rho_i$  such that

$$\inf_{\substack{x \in \bar{G}_i \cap \mathcal{X} \\ v \in \partial g_i(x)}} \|v\| \geq \rho_i > 0,$$



where  $\bar{G}_i = \{x : g_i(x) = 0\}$ , and  $\partial g_i(x) = \{v : g_i(y) - g_i(x) \geq v^\top(y - x), \forall y\}$  is the subdifferential of  $g_i$  at  $x$ .

**Assumption 4.** *There exist a constant  $\gamma > 0$  and a function  $h : [0, +\infty)^{l+m} \mapsto [0, +\infty)$  such that (a)  $h(\mathbf{0}) = 0$ , (b)  $h$  is nondecreasing in each argument, and (c) for all  $x \in \mathcal{X}$ ,*

$$d_{\mathcal{K}}(x) \leq \gamma h(d_{C_1}(x), \dots, d_{C_l}(x), d_{G_1}(x), \dots, d_{G_m}(x)), \quad (6)$$

where  $\mathbf{0}$  is the zero vector, and  $d_C(x) = \|x - \mathcal{P}_C(x)\|$  is the distance between  $x$  and  $C$ .

Assumption 2 is a common condition for objective functions. Assumption 3 is derived from Yang et al. (2017), and can also be easily verified given concrete  $g_i(x)$  functions. Assumption 4 is the key to transforming problem (5) into an unconstrained one, and to a great extent it needs to be analyzed case by case. Verifying Assumption 4 for the FPS problem is the main focus of Section 3.3. Define the function

$$\mathcal{L}(x; \mu) = f(x) + \mu h(d_{C_1}(x), \dots, d_{C_l}(x), \rho_1^{-1}[g_1(x)]_+, \dots, \rho_m^{-1}[g_m(x)]_+),$$

where  $[x]_+ = \max\{x, 0\}$ . Then the following theorem, which can be seen as a generalization to Proposition 2 of Kundu et al. (2018), states the equivalence between (5) and an unconstrained optimization problem  $\min_{x \in \mathcal{X}} \mathcal{L}(x; \mu)$ .

**Theorem 1.** *Suppose that Assumptions 2 to 4 hold, and define  $f_* = \min_{x \in \mathcal{K}} f(x)$  and  $\mathcal{L}_* = \min_{x \in \mathcal{X}} \mathcal{L}(x; \mu)$ . Also let  $x_\varepsilon \in \mathcal{X}$  be an approximate solution such that  $\mathcal{L}(x_\varepsilon; \mu) \leq \mathcal{L}_* + \varepsilon$  for  $\varepsilon > 0$ , and denote  $y_\varepsilon = \mathcal{P}_{\mathcal{K}}(x_\varepsilon)$ . Then the following conclusions hold: (a) if  $\mu \geq \gamma L$ , then  $f_* = \mathcal{L}_*$ ; (b) if  $\mu \geq \gamma(L + 1)$ , then  $\|x_\varepsilon - y_\varepsilon\| \leq \varepsilon$  and  $\mathcal{L}(y_\varepsilon; \mu) \leq \mathcal{L}_* + \varepsilon$ .*

### 3.3 The Gradient FPS Algorithm

The FPS problem (2) can be written in the form of (5) by defining  $f(X) = -\text{tr}(SX) + \lambda \|X\|_{1,1}$ ,  $C_1 = \{X : \text{tr}(X) = d\}$ ,  $g_1(X) = \theta_1(X) - 1$ ,  $g_2(X) = -\theta_p(X)$ ,  $G_1 = \{X : g_1(X) \leq 0\}$ ,  $G_2 = \{X : g_2(X) \leq 0\}$ ,  $\mathcal{K} = \mathcal{F}^d$ , and  $\mathcal{X} = \{X_{p \times p} : \|X\|_F \leq \sqrt{d}\}$ , where  $\|\cdot\|_F \equiv \|\cdot\|_{2,2}$  is the Frobenius norm. In the remaining part of this article, the above symbols are specific to the FPS model. To apply Theorem 1, we need to verify the three assumptions presented in Section 3.2, among which Assumption 4 plays a central role in developing the unconstrained optimization problem. The following theorem, which describes the geometry of the Fantope, is the key to validating that assumption.



**Theorem 2.** Let  $\mathcal{F}_1 = \{X_{p \times p} : \text{tr}(X) = d\}$  and  $\mathcal{F}_{2,3} = \{X_{p \times p} : O \preceq X \preceq I\}$ . If  $3 \leq d \leq (p-1)/2$ , then for any  $p \times p$  symmetric matrix  $X$ ,

$$d_{\mathcal{F}^d}(X) \leq \sqrt{p/(d+1)} \cdot d_{\mathcal{F}_1}(X) + \sqrt{p} \cdot d_{\mathcal{F}_{2,3}}(X). \quad (7)$$

Theorem 2 is proved using the theory of normal cones in convex analysis. With inequality (7), we are able to verify the required assumptions in the following corollary.

**Corollary 1.** For the FPS problem (2), if  $3 \leq d \leq (p-1)/2$ , then

1.  $f(X)$  satisfies Assumption 2 with  $L = \|S\|_F + \lambda p$ .
2. Assumption 3 holds with  $\rho_1 = 1/\sqrt{d}$  and  $\rho_2 = 1/\sqrt{p}$ .
3.  $d_{\mathcal{K}}(X) \leq \sqrt{p/(d+1)} (d_{C_1}(X) + \sqrt{d+1} \cdot d_{G_1}(X) + \sqrt{d+1} \cdot d_{G_2}(X))$ .

As a consequence, define

$$\mathcal{L}(X) = -\text{tr}(SX) + \lambda \|X\|_{1,1} + \mu (d_{C_1}(X) + r_1 [g_1(X)]_+ + r_2 [g_2(X)]_+), \quad (8)$$

and then  $\min_{X \in \mathcal{K}} f(X) = \min_{X \in \mathcal{X}} \mathcal{L}(X)$ , where  $\mu = (L+1)\sqrt{p/(d+1)}$ ,  $r_1 = \sqrt{d(d+1)}$ , and  $r_2 = \sqrt{p(d+1)}$ .

Since projection onto  $\mathcal{X}$  is trivial, (8) is essentially an unconstrained objective function, which can be minimized using any familiar subgradient method. However, subgradient methods for nonsmooth objective functions in general require  $\mathcal{O}(1/\varepsilon^2)$  iterations to achieve an optimization error of  $\varepsilon$ , which may be slow in practice. Below we introduce an efficient algorithm that only requires  $\mathcal{O}(1/\varepsilon)$  outer iterations. For convenience, define  $f_1(X) = \lambda \|X\|_1$  and  $f_2(X) = -\text{tr}(SX) + \mu d_{C_1}(X) + \mu r_1 [g_1(X)]_+ + \mu r_2 [g_2(X)]_+$ , so the problem becomes  $\min_{X \in \mathcal{X}} \mathcal{L}(X) := f_1(X) + f_2(X)$ . Then we apply the proximal-proximal-gradient method (Ryu and Yin, 2017), which evaluates the proximal operators for  $f_1$  and  $f_2$  iteratively. The outline of the proposed method, which we term as the gradient FPS algorithm, or GradFPS for short, is given in Algorithm 1.

We comment that the operations in Algorithm 1 are all inexpensive compared with a full eigen decomposition. First,  $\text{prox}_{\alpha f_1}(X) = \mathcal{S}_{\alpha\lambda}(X)$  is the elementwise soft-thresholding operator, which has a closed-form solution. We provide two algorithms for computing the proximal operator for  $f_2$ : one is a direct method, and the other is an iterative method. The details of the two algorithms are given in Appendix A.2.

---

**Algorithm 1** The gradient FPS (GradFPS) algorithm

---

**Input:**  $S, T, \alpha$ , initial value  $X_0 \in \mathcal{X}$

**Output:**  $\hat{X}$

- 1:  $Z_0^{(1)} = Z_0^{(2)} \leftarrow X_0$
  - 2: **for**  $k = 0, 1, \dots, T - 1$  **do**
  - 3:    $\bar{Z}_k \leftarrow (Z_k^{(1)} + Z_k^{(2)})/2$
  - 4:    $X_{k+1} \leftarrow \mathcal{P}_{\mathcal{X}}(\bar{Z}_k) = \min \left\{ 1, \sqrt{d}/\|\bar{Z}_k\|_F \right\} \cdot \bar{Z}_k$
  - 5:    $Z_{k+1}^{(1)} \leftarrow Z_k^{(1)} - X_{k+1} + \mathbf{prox}_{\alpha f_1}(2X_{k+1} - Z_k^{(1)})$
  - 6:    $Z_{k+1}^{(2)} \leftarrow Z_k^{(2)} - X_{k+1} + \mathbf{prox}_{\alpha f_2}(2X_{k+1} - Z_k^{(2)})$
  - 7: **end for**
  - 8: **return**  $\hat{X} = T^{-1} \sum_{k=1}^T X_k$
- 

### 3.4 Convergence Analysis

One remarkable benefit of the GradFPS algorithm is that we can bound its optimization error at any finite iteration step. With a sufficiently large number of iterations, Algorithm 1 can be shown to output an  $\varepsilon$ -optimal and  $\varepsilon$ -feasible solution  $\hat{X}$ , in the sense that  $\mathcal{L}(\hat{X}) \leq \mathcal{L}_* + \varepsilon$  and  $d_{\mathcal{K}}(\hat{X}) \leq \varepsilon$ . We develop the convergence property and an explicit upper bound for the optimization error in the following theorem.

**Theorem 3.** *The output  $\hat{X}$  of Algorithm 1 satisfies*

$$\mathcal{L}(\hat{X}) \leq \min_{X \in \mathcal{X}} \mathcal{L}(X) + \frac{C}{T} \quad \text{and} \quad d_{\mathcal{K}}(\hat{X}) \leq \frac{C}{T},$$

where  $C$  is a constant that only depends on  $S, X_0$ , and the model parameters. The explicit expression of  $C$  is given in Appendix A.1.

If the optimization problem  $\min_{X \in \mathcal{X}} \mathcal{L}(X)$  can be solved exactly, resulting in a solution  $\hat{X}_*$ , then the statistical property of  $\hat{X}_*$  has already been studied by Vu et al. (2013). However, in any practical implementation, only a finite-precision solution such as  $\hat{X}$  can be obtained.  $\hat{X}$  differs from the ideal  $\hat{X}_*$  in two aspects: it does not exactly minimize the objective function, and it is not necessarily within the constraint set  $\mathcal{K}$ . In Corollary 2, we show that despite the presence of such approximations,  $\hat{X}$  is still a good estimator for  $\Pi$ , and we explicitly give an upper bound of its estimation error as a function of the sample size  $n$  and the number of iterations  $T$ .

**Assumption 5.** *There exists a constant  $\sigma > 0$  such that  $\max_{i,j} P(|S_{ij} - \Sigma_{ij}| \geq u) \leq 2 \exp(-4nu^2/\sigma^2)$  for all  $u \leq \sigma$ .*

**Corollary 2.** *Suppose that Assumptions 1 and 5 hold, and take  $\lambda = \sigma \sqrt{\log(p)/n}$ . Then with probability at least  $1 - 2/p^2$ , we have*

$$\|\hat{X} - \Pi\|_F \leq \frac{4\sigma s \sqrt{\log(p)}}{\delta_d \sqrt{n}} + \frac{\sqrt{2C/\delta_d}}{\sqrt{T}} + \frac{C}{T}, \quad (9)$$

where  $C$  is given in Theorem 3.

The error bound (9) has an intuitive interpretation. The first term quantifies the *statistical error*, which depends on the  $\log(p)$  term that is common in high-dimensional data analysis. The second term is the *optimization error*, which decays at the  $\mathcal{O}(1/\sqrt{T})$  rate. The last term is the *feasibility error*, since  $\hat{X}$  is not necessarily a projection matrix.

## 4 Online Sparse PCA

### 4.1 Online Learning Setting

In this section we consider the scenario in which data are obtained in a streaming fashion. Streaming data reflect many practical needs that data acquisition and computation happen roughly at the same time. For instance, the complete data collection procedure may span a long period of time, or the data set is too large to be stored entirely on the machine. In both cases, it is desirable to make full use of the existing data, and then update the model parameters when new data points come in. Such algorithms are typically called online learning algorithms. Correspondingly, the algorithms that use the whole data set, for instance Algorithm 1, are referred to as offline learning or batch learning algorithms.

Formally, we assume that there is an infinite sequence of independent random vectors  $Z_1, Z_2, \dots \in \mathbb{R}^p$  with  $E(Z_t) = 0$  and  $Cov(Z_t) = E(S_t) = \Sigma$ ,  $t \geq 1$ , where  $S_t = Z_t Z_t^T$ . The true covariance matrix  $\Sigma$  has the same sparsity setting as the batch version, and the estimation target is the top- $d$  projection matrix  $\Pi$  of  $\Sigma$ . We define the online learning procedure as follows. At each time point  $t$ , the data analyst constructs an estimator  $X_t$  for  $\Pi$ . To match the nature of streaming data, we require that  $X_t$  only depends on  $Z_t$ ,  $X_{t-1}$ , and optionally some other quantities that depend on the history  $\{Z_i\}_{i=0}^t$  with a storage size not growing with  $t$ . The procedure stops at time  $T$ , and a final estimator  $\hat{X}_T$  is output by the online learning algorithm. For clarity,  $T$  is also called the sample size of the streaming data in this context.

The performance of an online algorithm is evaluated based on both the statistical and optimization properties. For the final output  $\hat{X}_T$ , we are interested in its estimation error  $\|\hat{X}_T - \Pi\|_F$ . And for the whole estimator sequence  $\{X_t\}$ , we also care about its cumulative optimization loss  $\mathcal{R}(\{X_t\}, T)$ , defined in the following way. After each  $X_t$  is constructed, we use it to predict a future data point  $Z_{t+1}$ , and define the loss function

$$\ell_t(X_t) = -Z_{t+1}^T X_t Z_{t+1} + \lambda \|X_t\|_{1,1} + \nu d_{\mathcal{K}}(X_t), \quad (10)$$

where  $\lambda$  and  $\nu$  are constants. In this loss function, the first term quantifies the (negative) explained variance on new data if  $X_t$  is treated as a projection matrix, the second term encourages the sparsity of  $X_t$ , and the third term penalizes the deviation from the constraint set  $\mathcal{K} = \mathcal{F}^d$ . For the whole procedure, define the total loss

$$\mathcal{R}(\{X_t\}, T) = \sum_{t=1}^T \ell_t(X_t) - \sum_{t=1}^T \ell_t(\Pi), \quad (11)$$

which describes the cumulative excess loss of  $\{X_t\}$  compared with the true projection matrix  $\Pi$ . In online learning literature, the function  $\mathcal{R}(\cdot)$  is typically called the *regret*. Naturally, a good online learning algorithm should have a strict control of the regret as a function of  $T$ . In the next two sections, we propose two different online sparse PCA algorithms based on the characteristics of the streaming data.

## 4.2 The Large-sample-size Case

The first case is the typical setting of streaming data, where new data are obtained with a high frequency. As a result, the sample size  $T$  is assumed to be much larger than the dimension  $p$ . The primary goal of the online learning algorithm is to make quick prediction  $X_t$  after the data point  $Z_t$  is observed, and meanwhile to control the regret and final estimation error.

Under this setting, we solve the online sparse PCA problem using the incremental proximal method (Bertsekas, 2011), which is a generalization to the simple subgradient method. Originally designed for batch optimization problems, the incremental proximal method is extended to the online setting in this article. We call the proposed algorithm Online-T GradFPS, to indicate that it is mostly used for streaming data that have a large sample size  $T$ . The outline of Online-T GradFPS is given in Algorithm 2.

Compared with Algorithm 1, Online-T GradFPS has a significantly lower computational cost per iteration, due to the following two reasons. First, the eigenvalues are computed for a sparse matrix  $X_t^{(1)}$ , since it is the output of a soft-thresholding opera-

---

**Algorithm 2** The Online-T GradFPS algorithm
 

---

**Input:**  $\{Z_t\}$ ,  $T$ ,  $\{\alpha_t\}$ , initial value  $X_0$

**Output:**  $\hat{X}_T$

- 1: **for**  $t = 1, \dots, T$  **do**
  - 2:  $X_t^{(0)} \leftarrow X_{t-1}$
  - 3:  $X_t^{(1)} \leftarrow \mathcal{S}_{\alpha_t \lambda}(X_t^{(0)})$
  - 4:  $X_t^{(2)} \leftarrow X_t^{(1)} - \alpha_t \nu \sqrt{pd} \mathbf{1}\{\theta_1 > 1\} \gamma_1 \gamma_1^\top + \alpha_t \nu p \mathbf{1}\{\theta_p < 0\} \gamma_p \gamma_p^\top$ ,  
 where  $\theta_i = \theta_i(X_t^{(1)})$ ,  $\gamma_i = \gamma_i(X_t^{(1)})$ ,  $i = \{1, p\}$
  - 5:  $X_t^{(3)} \leftarrow X_t^{(2)} + \min\{\beta, 1\} \cdot s \cdot I$ , where  $s = (d - \text{tr}(X_t^{(2)}))/p$ ,  $\beta = \alpha_t \nu / \{(d+1)|s|\}$
  - 6:  $X_t \leftarrow \mathcal{P}_{\mathcal{X}} \left( X_t^{(3)} + \alpha_t S_t \right) = \min \left\{ 1, \sqrt{d} / \|X_t^{(3)} + \alpha_t S_t\|_F \right\} \cdot \left( X_t^{(3)} + \alpha_t S_t \right)$
  - 7: **end for**
  - 8: **return**  $\hat{X}_T = T^{-1} \sum_{t=1}^T X_t$
- 

tor. Computing the extreme eigenvalues for  $X_t^{(1)}$  is much more efficient than for a dense matrix, since its complexity depends on the number of nonzero elements. Second, only the largest and smallest eigenvalues of  $X_t^{(1)}$  need to be calculated, which further saves the computation time.

The following theorem shows that if  $\|S_t\|_F$  is properly bounded, then the average regret of Algorithm 2 decays at the rate of  $\mathcal{O}(1/\sqrt{T})$ , which matches the best known result for the online subgradient method on a non-strongly convex objective function.

**Assumption 6.** (a) The sequence  $\xi_t = \|S_t - \Sigma\|_F$ ,  $t \geq 1$  is independent and identically distributed, with a sub-exponential distribution. (b) The sequence  $\zeta_t = \|S_t\|_F^2$  is also sub-exponential. Specifically, there exist constants  $b_1, b_2, \sigma_1, \sigma_2 \geq 0$  such that

$$\begin{aligned} E[\exp\{\lambda(\xi_t - \mu_1)\}] &\leq \exp(\lambda^2 \sigma_1^2 / 2), \quad \forall |\lambda| \leq 1/b_1, \\ E[\exp\{\lambda(\zeta_t - \mu_2)\}] &\leq \exp(\lambda^2 \sigma_2^2 / 2), \quad \forall |\lambda| \leq 1/b_2, \end{aligned}$$

where  $\mu_1 = E(\xi_t)$  and  $\mu_2 = E(\zeta_t)$ .

**Theorem 4.** Let  $\alpha_1 = \alpha_0 > 0$  and  $\alpha_t = \alpha_0 / \sqrt{t-1}$  for  $t \geq 2$ . Then the following conclusions hold:

1. (Optimization regret bound) If  $\|S_t\|_F$  is bounded, then  $T^{-1} \mathcal{R}(\{X_t\}, T) = \mathcal{O}(p^2 / \sqrt{T})$ .

2. (Statistical estimation error) *If Assumptions 1 and 6 hold, and  $\nu \geq \lambda p + \|\Sigma\|_F + 1$ , then for any fixed  $\varepsilon \in (0, 1)$ ,*

$$\|\hat{X}_T - \Pi\|_F = \mathcal{O}\left(\sqrt{(\log(1/\varepsilon) + \nu^2 p^2)/\sqrt{T} + \lambda s}\right)$$

*holds with probability at least  $1 - \varepsilon$ .*

*The explicit expressions of  $\mathcal{R}(\{X_t\}, T)$  and  $\|\hat{X}_T - \Pi\|_F$  are given in Appendix A.1.*

Theorem 4 indicates that  $\lambda$  needs to be set small if the primary goal is to use the final output  $\hat{X}_T$  for estimation. Otherwise, a moderate  $\lambda$  leads to more sparse intermediate results and is thus better for interpretation. The estimation error bound also implies that Online-T GradFPS has a slower convergence rate than the batch GradFPS with respect to the sample size. However, as has been explained previously, the major advantage of Online-T GradFPS is its computational efficiency, which offsets its weakness in estimation error.

### 4.3 The High-dimensional Case

When the data dimension  $p$  is much larger than the sample size  $T$ , the method in Section 4.2 is no longer applicable, since both the regret of  $\{X_t\}$  and the estimation error of  $\hat{X}_T$  depend on a polynomial of  $p$ . As a comparison, in high-dimensional statistical analysis, such quantities usually depend on  $\log(p)$  under suitable sparsity assumptions. Therefore, we are motivated to consider alternative optimization schemes that result in a smaller regret and a better statistical accuracy, possibly at the expense of larger computational cost in each iteration.

For general online learning problems, one of the most natural and straightforward methods to obtain  $X_t$  is to apply the batch algorithm on all collected data  $S_1, \dots, S_t$  up to time  $t$ . Such a scheme is known as the follow-the-leader (FTL) algorithm. For online sparse PCA, the FTL algorithm is a valid online learning algorithm, since the matrix  $S_{1:t} = t^{-1} \sum_{i=1}^t S_i$  can be computed with a constant storage. However, the main problem of FTL is its weak control of the regret, as the numerical experiment shows in Section 5. Intuitively, FTL focuses too much on the existing data, and leaves little room for the exploration of future observations.

Instead, we develop our online sparse PCA algorithm based on the generalized online mirror descent framework (OMD, Orabona et al., 2015). The key merit of the generalized OMD method is to replace the Frobenius norm  $\|S_t\|_F$  in the error bound (13) by the infinity norm  $\|S_t\|_{\infty, \infty}$ , which only grows at the speed of  $\log(p)$  under some

---

**Algorithm 3** The Online-P GradFPS algorithm

---

**Input:**  $\{S_t\}, \{\varepsilon_t\}, T, \lambda$ **Output:**  $\hat{X}$ 

- 1:  $Y_0 \leftarrow O$
  - 2: **for**  $t = 1, \dots, T$  **do**
  - 3:    $Y_t \leftarrow Y_{t-1} + S_t$
  - 4:   Find  $X_t \in \mathcal{X}$  such that  $\mathring{\mathcal{L}}(X_t; Y_t, t) \leq \mathring{\mathcal{L}}_* + \beta\sqrt{t}\varepsilon_t^2/2$ ,  
      where  $\mathring{\mathcal{L}}_* = \min_{X \in \mathcal{X}} \mathring{\mathcal{L}}(X; Y_t, t)$
  - 5: **end for**
  - 6: **return**  $\hat{X}_T = X_T$
- 

regularity conditions. Due to this reason, the proposed algorithm is named as Online-P GradFPS, to emphasize that it is more suitable for a large  $p$ .

For brevity, we set the constants  $r = \log(p)/\{\log(p) - 1\}$  and  $\beta = \exp(-4)/\{\log(p) - 1\}$ , and define the function

$$\begin{aligned} \mathring{\mathcal{L}}(X; Y, t) = & -\text{tr}(YX) + \lambda t \|X\|_{1,1} + \sqrt{t} \|X\|_{r,r}^2/2 \\ & + (L_t + 1) \sqrt{p/(d+1)} (d_{C_1}(X) + r_1[g_1(X)]_+ + r_2[g_2(X)]_+), \end{aligned} \quad (12)$$

where  $L_t = \|Y\|_F + \lambda t p + \exp(-4)\sqrt{td}p^2$ . We reuse the notation in Section 3.3 for other terms in (12). The main steps of Online-P GradFPS are given in Algorithm 3. It is worth mentioning that we improve the original OMD method by allowing an approximate solution for the subproblem in each iteration (line 4 of Algorithm 3), which is more realistic and efficient in practice. Solving the subproblem of Algorithm 3 is very similar to that of Algorithm 1, and we provide the details in Appendix A.3.

Similar to the large-sample-size case, the following theorem describes both the optimization error and the statistical accuracy of Algorithm 3.

**Theorem 5.** *The following conclusions hold:*

1. (Optimization regret bound) If  $\|S_t\|_{\infty, \infty}$  is bounded and  $\varepsilon_t = \mathcal{O}(1/\sqrt{t})$ , then  $T^{-1}\mathcal{R}(\{X_t\}, T) = \mathcal{O}(1/\sqrt{T})$ .
2. (Statistical estimation error) If Assumptions 1 and 5 hold,  $\lambda = \sigma\sqrt{\log(p)/T}$ , and



$\varepsilon_t = 1/\sqrt{t}$ , then with probability at least  $1 - 2/p^2$ , we have

$$\|\hat{X}_T - \Pi\|_F = \mathcal{O}\left(\frac{s\sqrt{\log(p)} + s^{2-4/\log(p)}}{\sqrt{T}}\right).$$

The explicit expressions of  $\mathcal{R}(\{X_t\}, T)$  and  $\|\hat{X}_T - \Pi\|_F$  are given in Appendix A.1.

Comparing the results in Theorem 5 and those in Theorem 4, it is clear that the optimization errors of the two algorithms have the same order for  $T$ , but the estimation error of Online-P GradFPS decays faster than that of Online-T GradFPS. The price for the better estimation accuracy is a larger computational cost per iteration, which will be made clear in the simulation study.

## 5 Simulation Study

### 5.1 Simulation Setting

In this section we conduct a number of numerical experiments to evaluate the performance of the sparse PCA algorithms proposed in this article. The problem setting is as follows. We assume that the data  $Z_1, \dots, Z_n$  follow independent and identically distributed multivariate normal distribution  $N(0, \Sigma)$ , where  $\Sigma$  is the true covariance matrix of  $p$  variables, and  $n$  is the sample size. For online learning algorithms, the data sequence is of infinite length, and the online algorithm will choose a terminal sample size  $T$ . The  $p$  variables are categorized into three groups: the first signal group contains  $d_1 = 20$  variables, the second signal group contains  $d_2 = 15$  variables, and the last noise group consists of  $(p - d_1 - d_2)$  noise variables. Figure 1(a) gives a visualization of the true covariance matrix  $\Sigma$  with  $p = 100$ , which shows that most variables are weakly correlated with each other, but the ones within the same signal group have higher correlations. In different experiments,  $n$  and  $p$  may vary, but  $d_1$  and  $d_2$  are kept fixed.

The  $\Sigma$  matrix is obtained by generating the eigenvalues  $\Lambda$  and eigenvectors  $Q$  in the following way. Let  $U_{r_1:r_2, c_1:c_2}$  denote the submatrix of a  $p \times p$  matrix  $U$ , with row indices  $r_1$  to  $r_2$  and column indices  $c_1$  to  $c_2$ . When  $r_1 = r_2$  or  $c_1 = c_2$ , a single index is used. First simulate a  $U$  matrix such that  $U_{1:d_1, 1} \stackrel{iid}{\sim} Unif(0.9, 1.1)$ ,  $U_{(d_1+1):p, 1} = 0$ ,  $U_{1:d_1, 2} = U_{(d_1+d_2+1):p, 2} = 0$ ,  $U_{(d_1+1):(d_1+d_2), 2} \stackrel{iid}{\sim} Unif(0.9, 1.1)$ , and  $U_{1:p, 3:p} \stackrel{iid}{\sim} N(0, 1)$ . Then a QR decomposition is performed as  $U = QR$ , and  $Q$  is used as the eigenvectors of  $\Sigma$ . Next, let  $\Lambda = \text{diag}\{12, 6, \lambda_3, \dots, \lambda_p\}$ , where  $\lambda_i \stackrel{iid}{\sim} Unif(0, 2)$ , and then  $\Sigma$  is computed as  $\Sigma = Q\Lambda Q^T$ . Figure 1(b) shows the first five columns of  $Q$ , and clearly the first  $d = 2$  columns of  $Q$  contain the sparse eigenvectors.

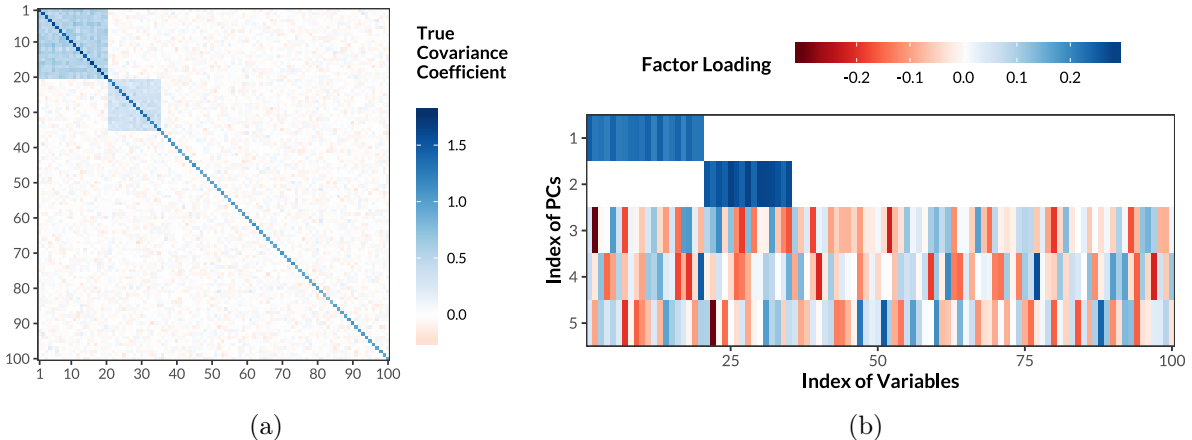


Figure 1: (a) The true covariance matrix  $\Sigma$  with  $p = 100$ . (b) The eigenvectors of  $\Sigma$  associated with the five largest eigenvalues.

## 5.2 Batch Algorithms

The first experiment compares the computational efficiency of the existing ADMM-based algorithm (ADMM-FPS, [Vu et al., 2013](#)) and the proposed GradFPS (Algorithm 1) with different sizes of data. Under each pair of  $(n, p)$ , a data set  $Z_1, \dots, Z_n$  is simulated to compute the sample covariance matrix  $S = n^{-1} \sum_{i=1}^n Z_i Z_i^T$ , and the sparsity parameter is set to  $\lambda = 0.5 \sqrt{\log(p)/n}$ . We compute the estimator  $\hat{X}$  using both algorithms with initial value  $X_0 = V_2 V_2^T$ , where  $V_2$  contains the top two eigenvectors of  $S$ . For both algorithms, the best step size parameter is chosen by trying ten equally-spaced values ranging from 0.01 to 0.1. We then plot the estimation error in each iteration against the computing time, with the comparison results illustrated in Figure 2.

Figure 2 shows a number of interesting findings. First, as expected, GradFPS has demonstrated superior computational efficiency compared with ADMM-FPS. It is clear that the curves for GradFPS decrease very quickly at early stages of the optimization, which indicates that GradFPS is able to provide reasonably accurate solutions in a short time. Such a property is crucial, since a common practice for computing sparse PCA is to use convex solutions as good initial values for fast nonconvex methods ([Wang et al., 2014](#); [Chen and Wainwright, 2015](#); [Tan et al., 2018](#)). Second, the curves for ADMM-FPS have irregular shapes, containing some long “plateaus” and even increasing parts. In practice, such patterns are misleading for convergence tests. In contrast, the curves for GradFPS mostly show a monotone progress. Finally, even if the same initial value is supplied to both algorithms, the GradFPS algorithm tends to make better use of it,

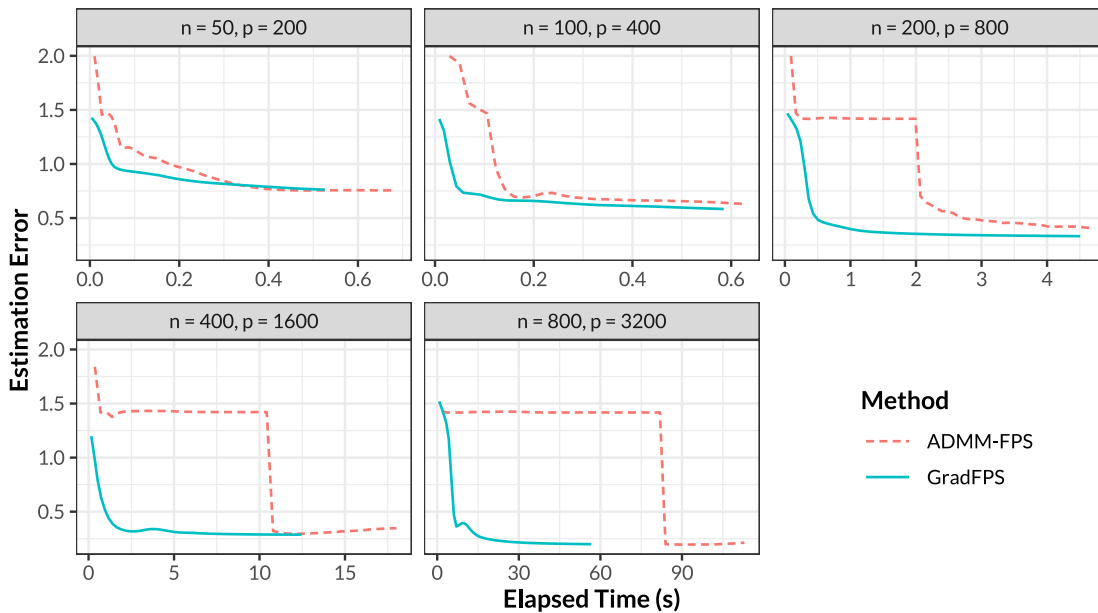


Figure 2: Comparing the computational efficiency of the existing ADMM-based algorithm and the proposed GradFPS. The horizontal axis is the elapsed time in seconds, and the vertical axis stands for the estimation error  $\|\hat{X} - \Pi\|_F$ .

as the initial errors of GradFPS are smaller than those of ADMM-FPS.

### 5.3 Online Algorithms

The next experiment studies the behavior of Online-P GradFPS (Algorithm 3) for online sparse PCA, compared with the naive FTL algorithm. In this case  $T = 100$ ,  $p = 400$ , and data points  $Z_1, \dots, Z_{T+1} \stackrel{iid}{\sim} N(0, \Sigma)$  are drawn in a streaming fashion. We apply the FTL method and Online-P GradFPS on this data sequence, and compute their regret values at each time point. To account for the variability in the data generation process, this experiment is repeated ten times, and Figure 3(a) and Figure 3(b) show the cumulative and average regret values for the two online algorithms, respectively.

It is clear from Figure 3 that Online-P GradFPS has much smaller regret values compared with the naive FTL method. In fact, at the final time point Online-P GradFPS only has about half of the regret value of FTL. This result implies that the proposed method is effective in controlling the procedural loss.

### 5.4 Comparison between Online-T and Online-P Algorithms

In Section 4 we have developed two different online sparse PCA algorithms, so a natural question is how they compare to each other. To answer this, we fix  $p = 200$  and simulate

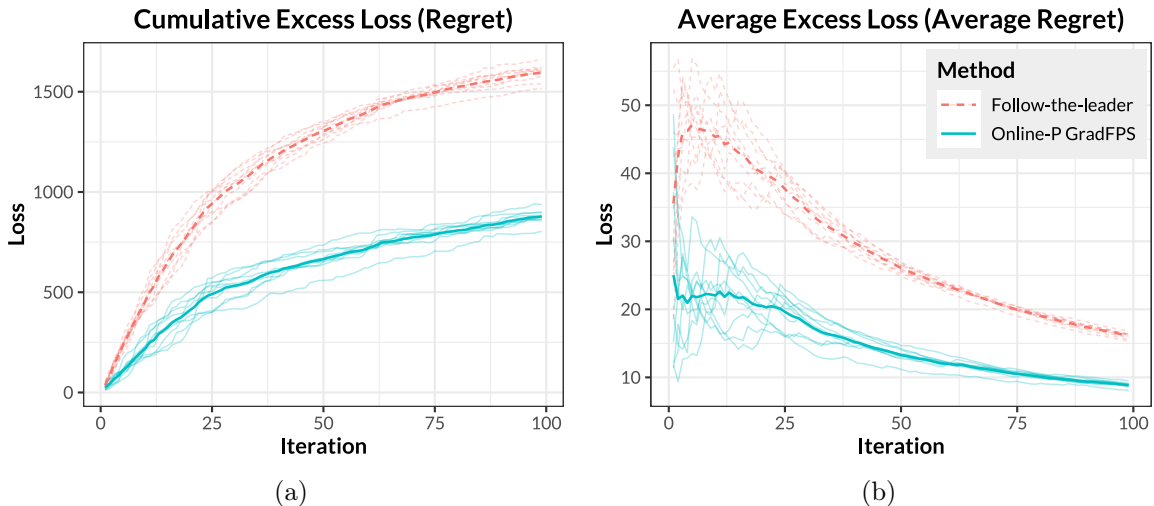


Figure 3: (a) The cumulative regret values for the two online algorithms. (b) The average regret values. Thin curves represent ten replications of the experiment, and thick ones stand for the mean value across experiments.

ten streaming data sets using the model in Section 5.1. Both the Online-T and Online-P GradFPS algorithms are applied to the data sets, with the former stopped after  $T_1 = 1000$  iterations, and the latter stopped at  $T_2 = 200$ . The estimation error at each iteration for both algorithms are shown in Figure 4(a).

It is clear that the convergence of Online-P GradFPS is much faster than Online-T GradFPS in terms of the number of iterations, which is consistent with the theory developed in Section 4. However, if the  $x$ -axis is set to the computing time, as illustrated in Figure 4(b), then we find that Online-T GradFPS is an order of magnitude faster. This phenomenon suggests the following guideline for choosing the online algorithm: if the number of data points are limited and the statistical accuracy is a concern, then Online-P GradFPS is preferred; otherwise, if data are abundant and computation needs to be fast, then Online-T GradFPS would be a proper choice.

## 6 Application

In this section we apply sparse PCA to an RNA sequencing data set to analyze the co-expression relationship among genes. The aim of our analysis is to detect groups of genes, typically referred to as modules, with high co-expression. Such an analysis is motivated by the biological conjecture that genes in the same module are likely to be functionally related (Stuart et al., 2003). Sparse PCA is well suited to this challenging

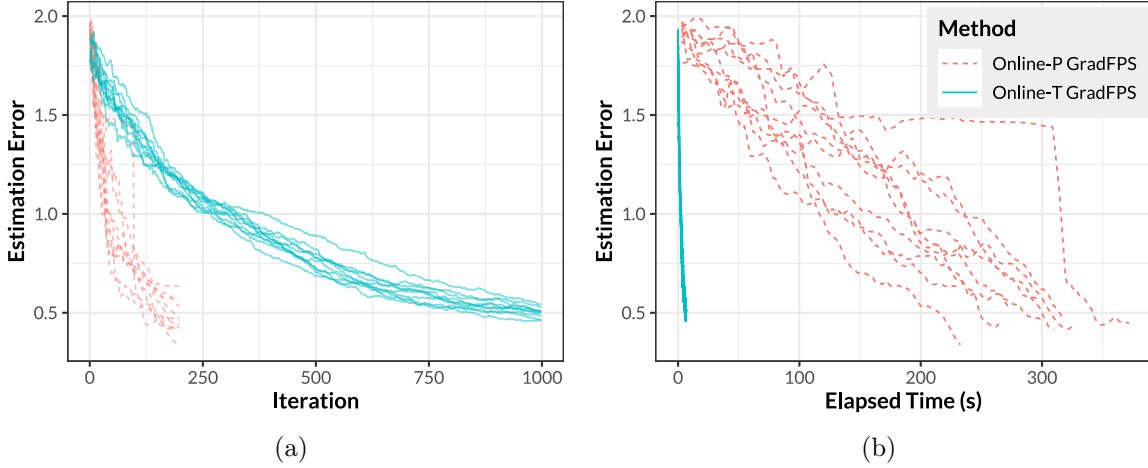


Figure 4: (a) Plotting the estimation error  $\|X_t - \Pi\|_F$  against the iteration index  $t$ . (b) The error versus the computing time. Each curve stands for one simulation run.

problem for which expression data are available for tens of thousands of genes.

We study the brain gene expression data collected by the CommonMind Consortium (CMC), which contain  $p = 16,423$  genes from 258 schizophrenia (SCZ) subjects and 279 control subjects (Fromer et al., 2016). The control group is used as a baseline, and our main interest is in the SCZ group. We compute Pearson’s correlation coefficients between genes utilizing the processed and normalized expression data provided by the CMC, and then apply sparse PCA to the sample correlation matrix. The number of sparse principal components is chosen to be  $d = 5$ , and the sparsity parameter  $\lambda$  is selected in the following way. First, we compute the solution paths of sparse PCA in both the SCZ group and the control group based on a common sequence of  $\lambda$  values. Then for each  $\lambda$ , two active sets  $\Omega_{ctr}^\lambda, \Omega_{scz}^\lambda \subset \{1, 2, \dots, p\}$  are determined, where  $i \in \Omega_{ctr}^\lambda$  if the  $i$ -th gene has at least one nonzero factor loading in the five sparse principal components, and  $i \in \Omega_{scz}^\lambda$  is defined likewise. We limit the range of  $\lambda$  so that  $\min\{|\Omega_{ctr}^\lambda|, |\Omega_{scz}^\lambda|\} \geq 50$  and  $\max\{|\Omega_{ctr}^\lambda|, |\Omega_{scz}^\lambda|\} \leq 300$ , where  $|\Omega|$  denotes the cardinality of a set  $\Omega$ . Define the overlapping coefficient as  $V(\lambda) = |\Omega_{ctr}^\lambda \cap \Omega_{scz}^\lambda| / |\Omega_{ctr}^\lambda \cup \Omega_{scz}^\lambda|$ , and  $\lambda$  is chosen to maximize  $V(\lambda)$ , indicating that these two groups share maximal common structures. Using this approach, we finally select  $\lambda = 0.85$ , under which  $|\Omega_{ctr}^\lambda| = 292$ ,  $|\Omega_{scz}^\lambda| = 185$ , and  $|\Omega_{ctr}^\lambda \cap \Omega_{scz}^\lambda| = 114$ .

After computing the sparse PCA solution for the SCZ group at the selected  $\lambda$ , the genes in the active set are clustered based on their factor loadings, with the number of clusters set to  $k = 5$ . For display, the indices of genes are reordered so that the genes in

the same cluster are adjacent. Figure 5 shows the sample correlation matrix and factor loadings based on the reordered indices of selected genes.

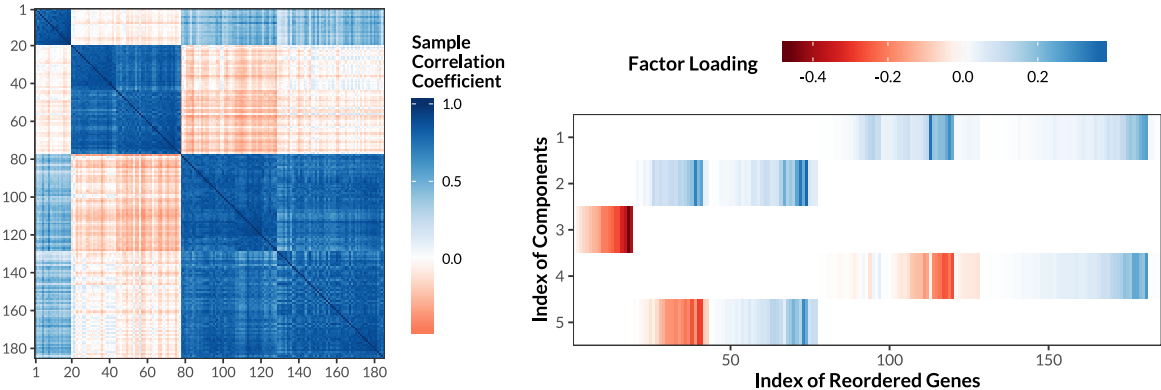


Figure 5: The reordered sample correlation matrix of the selected genes in the SCZ group (left) and the reordered factor loadings (right).

It can be easily observed from Figure 5 that there are three major modules in the correlation matrix, and the second and third modules have two sub-modules, respectively, resulting in five clusters in total. Such a structure is clearly reflected in the factor loadings, in which the first three components define the major modules, whereas the last two components add sub-structure to the second and third modules.

To validate our results, we compare the clusters reflected in Figure 5 with the modules obtained by the weighted gene co-expression network analysis (WGCNA, Zhang and Horvath, 2005). Table 1 demonstrates the cross table for the two methods of module assignment on the selected genes, where the numbered modules are given by our approach, and the ones labeled by color names are the WGCNA results provided by Fromer et al. (2016). It is clear that our modules are well aligned with the WGCNA ones, with three extra advantages. First, our clusters have smaller sizes and stronger within-group correlation. For instance, the Green WGCNA module contains 414 genes, whereas our M-1, a subset of the Green module, has only 19 genes. In many studies, researchers are more interested in a small number of genes that are representative for the whole module. Second, we have detected highly correlated genes that are assigned to different modules by WGCNA. As an example, the two genes in the Tan module are highly correlated with other M-4 genes (a subset of Turquoise), with average sample correlation coefficients 0.817 and 0.794, respectively. Finally, our clusters have revealed sub-structure within large modules, for example M-2 and M-3 are sub-modules for Brown.

Table 1: Cross table for sparse-PCA-based modules (row) and the WGCNA modules (column). The numbers in the parentheses stand for the sizes of WGCNA modules.

	Green (414)	Brown (528)	Turquoise (1155)	Tan (248)	Blue (609)
M-1	19	0	0	0	0
M-2	0	24	0	0	0
M-3	0	34	0	0	0
M-4	0	0	49	2	0
M-5	0	0	53	0	4

Next, by comparing with the control group, we study the structural change of gene co-expression relationship in the SCZ group. Consider the genes that are selected in the SCZ group but not in the control group, forming the gene set  $\Omega_{scz}^U = \Omega_{scz} \setminus \Omega_{ctr}$ . Figure 6 illustrates the sample correlation matrices on  $\Omega_{scz}^U$  for both the control group (left panel) and the SCZ group (middle panel). In addition, to better visualize the correlation pattern, density curves of off-diagonal correlation coefficients are shown in the right panel of Figure 6.

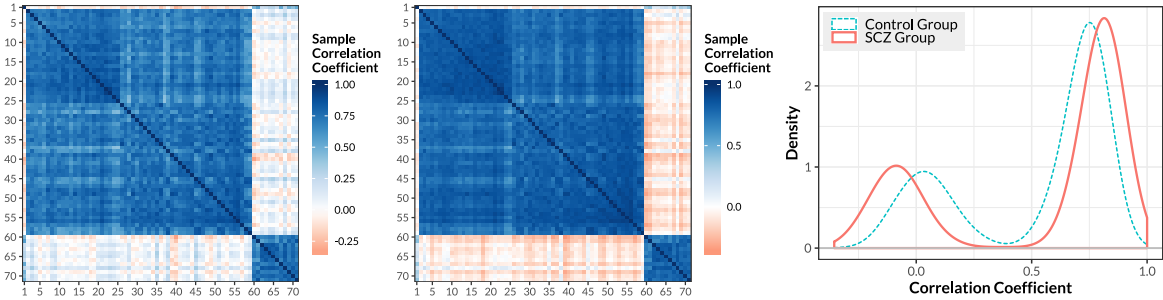


Figure 6: Comparison of correlation matrices on SCZ-group-specific genes  $\Omega_{scz}^U$ . Left: the correlation matrix on  $\Omega_{scz}^U$  for the control group. Middle: the correlation matrix for the SCZ group. Right: density curves for the off-diagonal correlation coefficients.

Figure 6 highlights an interesting difference between the control group and the SCZ group. In both groups, the correlation matrices indicate a similar two-block structure, but density curves of the correlations summarize the differences between groups. Both exhibit two modes, representing the between-module and within-module correlation coefficients, respectively; however, the coefficients in the SCZ group are obviously more extreme than those in the control group. The first mode differs in sign, indicating that the small positive between-module correlations in the control group are largely negative



in the SCZ group. These findings provide insights for future studies of schizophrenia based on brain gene expression data.

## 7 Conclusion and Discussion

In this article we have developed a novel efficient algorithm for the convex sparse PCA model, which is shown to outperform the existing ADMM-based method in many aspects. The main technique used is to transform the original highly constrained optimization problem into an unconstrained one, so that gradient-based and projection-free algorithms can be applied to seek the solution. This technique also allows us to compute sparse PCA for large-scale streaming data, leading to various online learning algorithms.

We point out that this framework of analysis has a great potential for further extensions, and below we mention two possible future directions for research. First, within the sparse PCA framework, the efficient algorithm can be developed for other types of problems that come with a different penalty term, such as the trend filtering ([Tibshirani, 2014](#)) or the localized functional PCA ([Chen and Lei, 2015](#)). Other types of penalty terms are also applicable as long as they are convex functions. Second, the two technical tools developed in this article, namely the gradient-based and projection-free optimization method for highly constrained problems, and the analysis of online learning algorithms, can be extended to other interesting statistical models. An example of this kind is the graphical lasso ([Friedman et al., 2008](#)), in which the precision matrix is constrained in the positive semidefinite cone with an elementwise  $\ell_1$  penalty. Similar to sparse PCA, online learning algorithms may be developed for graphical lasso using an unconstrained formulation of the objective function.

## Acknowledgments

This work was supported by NIMH grants R37MH057881-22 and R37MH057881-22S, and NSF grant DMS-1553884.

Data were generated as part of the CommonMind Consortium supported by funding from Takeda Pharmaceuticals Company Limited, F. Hoffman-La Roche Ltd and NIH grants R01MH085542, R01MH093725, P50MH066392, P50MH080405, R01MH097276, RO1-MH-075916, P50M096891, P50MH084053S1, R37MH057881, AG02219, AG05138, MH06692, R01MH110921, R01MH109677, R01MH109897, U01MH103392, and contract HHSN271201300031C through IRP NIMH. Brain tissue for the study was obtained from the following brain bank collections: the Mount Sinai NIH Brain and

Tissue Repository, the University of Pennsylvania Alzheimer’s Disease Core Center, the University of Pittsburgh NeuroBioBank and Brain and Tissue Repositories, and the NIMH Human Brain Collection Core. CMC Leadership: Panos Roussos, Joseph Buxbaum, Andrew Chess, Schahram Akbarian, Vahram Haroutunian (Icahn School of Medicine at Mount Sinai), Bernie Devlin, David Lewis (University of Pittsburgh), Raquel Gur, Chang-Gyu Hahn (University of Pennsylvania), Enrico Domenici (University of Trento), Mette A. Peters, Solveig Sieberts (Sage Bionetworks), Thomas Lehner, Stefano Marengo, Barbara K. Lipska (NIMH).

## A Appendix

### A.1 Expressions for constants and bounds

**Theorem 3:** The constant is  $C = \max\{\alpha^{-1}(C_0^2 + 4C_0L_g), 2C_0L_g\} + 2C_0L_g$ , where

$$L_g = \sqrt{(\lambda p)^2 + \{\|S\|_F + \mu(1 + \sqrt{(p+d)(d+1)})\}^2},$$

and  $C_0 > 0$  is a constant that only depends on  $X_0$  and the optimal point of the optimization problem.

**Theorem 4:** The regret bound in explicit form is given by

$$\frac{1}{T}\mathcal{R}(\{X_t\}, T) \leq \frac{2d/\alpha_0 + \alpha_0 C_2}{\sqrt{T}} + \frac{\alpha_0}{2T} \sum_{t=1}^T \frac{\|S_{t+1}\|_F^2 + C_1\|S_{t+1}\|_F}{\sqrt{t}}, \quad (13)$$

and the estimation error bound is  $\|\hat{X}_T - \Pi\|_F \leq C(T) + \sqrt{2/\delta_d} \cdot \sqrt{C(T) + \lambda s\sqrt{d}}$ , where  $C(T) = C_3/\sqrt{T} + C_4\{\log(T) + 1\}/T = \mathcal{O}(1/\sqrt{T})$ . The relevant constants are

$$\begin{aligned} C_1 &= \lambda p + \nu\sqrt{p(p+d)} + \nu\sqrt{p/(d+1)}, \\ C_2 &= \nu^2 p(p+d) + 2(\lambda p)^2 + 2\lambda p\nu\sqrt{p(p+d)} + 2\nu\sqrt{p/(d+1)}C_1, \\ C_3 &= 2d/\alpha_0 + D_1 + \alpha_0\{C_2 + C_1(\mu_1 + \|\Sigma\|_F) + \mu_2\}, \\ C_4 &= \alpha_0(C_1D_2 + D_3)/2, \end{aligned}$$

where  $D_1 = \max\{2b_1\varepsilon_l, 2\sigma_1\sqrt{2d\varepsilon_l}\}$ ,  $D_2 = \max\{2b_1\varepsilon_l, \sigma_1\sqrt{2\varepsilon_l}\}$ ,  $D_3 = \max\{2b_2\varepsilon_l, \sigma_2\sqrt{2\varepsilon_l}\}$ , and  $\varepsilon_l = \log(3/\varepsilon)$ .

**Theorem 5:** The regret bound in explicit form is given by

$$\frac{1}{T}\mathcal{R}(\{X_t\}, T) \leq \frac{\|\Pi\|_{r,r}^2}{2\sqrt{T}} + \frac{1}{T} \sum_{t=1}^T \left\{ (\psi_{t+1} + \lambda)\varepsilon_t + \frac{\beta\nu\sqrt{t\varepsilon_t^2}}{2} \right\} + \frac{1}{2\beta T} \sum_{t=1}^T \frac{\psi_{t+1}^2}{\sqrt{t}},$$

where  $\psi_t = \|S_t\|_{\infty, \infty}$ . The bound for the estimation error is

$$\|\hat{X}_T - \Pi\|_F \leq \frac{4\sigma s \sqrt{\log(p)} + 2s^{2-4/\log(p)} \sqrt{d}}{\delta_d \sqrt{T} + \beta} + \frac{\beta}{2\sqrt{T}} + \frac{\sqrt{\beta/(\delta_d + \beta/\sqrt{T})}}{T^{3/4}}.$$

## A.2 Computation of $\mathbf{prox}_{\alpha f_2}(X)$

By definition  $\mathbf{prox}_{\alpha f_2}(X) = \arg \min_{U \in \mathcal{X}} \{f_2(U) + (2\alpha)^{-1} \|U - X\|_F^2\}$ , so an easy iterative method has the form  $U_{k+1} = \mathcal{P}_{\mathcal{X}}(U_k - \alpha \eta_k \nabla f_2(U_k) - \eta_k(U_k - X))$ , where  $\eta_k$  is the step size. Since the objective function is strongly convex, this method converges at the speed of  $\mathcal{O}(1/K)$ , where  $K$  is the number of iterations.

The direct method for computing  $\mathbf{prox}_{\alpha f_2}(X)$  is based on the following observation. Let  $\theta_1 \geq \dots \geq \theta_p$  be the eigenvalues of  $X$ , and  $\gamma_1, \dots, \gamma_p$  be the associated eigenvectors. If  $\mu$  is sufficiently large, then  $\mathbf{prox}_{\alpha f_2}(X) = \sum_{i=1}^p u_i \gamma_i \gamma_i^T$ , where

$$u = (u_1, \dots, u_p)^T = \arg \min_{\substack{u_1 + \dots + u_p = d \\ 0 \leq u_i \leq 1}} \sum_{i=1}^p \left\{ -\theta_i u_i + \frac{1}{2\alpha} (\theta_i - u_i)^2 \right\} \quad (14)$$

is the solution to a quadratic programming problem. Most importantly, the elements in  $u$  has a decreasing order,  $u_1 \geq \dots \geq u_p$ , and for some index  $t$  we have  $u_i = 0$  for  $i \geq t$ . Therefore, we can sequentially compute the eigenvalues  $\theta_1 \geq \dots \geq \theta_t$  until  $u_t = 0$  is met. In this way the full decomposition of  $X$  is avoided.

## A.3 Solving the subproblem of Algorithm 3

Denote  $S_{1:t} = t^{-1} Y_t = t^{-1} \sum_{i=1}^t S_i$  and  $\mu_t = (\|S_{1:t}\|_F + \lambda p + \exp(-4) \sqrt{d/tp^2 + 1}) \sqrt{p/(d+1)}$ , and then we have  $\min_{X \in \mathcal{X}} \mathcal{L}(X; Y_t, t) = \min_{X \in \mathcal{X}} \{f_1(X) + f_2(X) + f_3(X)\}$ , where  $f_1(X) = \lambda \|X\|_1$ ,  $f_2(X) = -\text{tr}(S_{1:t} X) + \mu_t (d_{C_1}(X) + r_1 [g_1(X)]_+ + r_2 [g_2(X)]_+)$ , and  $f_3(X) = \|X\|_{r,r}^2 / (2\sqrt{t})$ . The subproblem of Algorithm 3 can be solved using the procedure in Algorithm 4.

The proximal operator  $\mathbf{prox}_{\alpha f_1}$  has closed-form solution  $\mathbf{prox}_{\alpha f_1}(X) = \mathcal{S}_{\alpha\lambda}(X)$ . The computation for  $\mathbf{prox}_{\alpha f_2}$  is given in Appendix A.2. The last operator  $\mathbf{prox}_{\alpha f_3}$  requires solving the problem  $\min_{X \in \mathcal{X}} \{\|X\|_{r,r}^2 / (2\sqrt{t}) + \|X - V\|_F^2 / (2\alpha)\}$ , which can be accomplished using the coordinate descent method.

## A.4 Proof of Theorem 1

We first prove an important fact: under Assumption 3,  $[g_i(x)]_+ \geq \rho_i d_{G_i}(x)$  for all  $x \in \mathcal{X}$ ,  $i = 1, \dots, m$ . This result was briefly given in Mahdavi et al. (2012) with a stronger

---

**Algorithm 4** Solving  $\min_{X \in \mathcal{X}} \hat{\mathcal{L}}(X; Y_t, t)$

---

**Input:**  $Y_t, K, \alpha$ , initial value  $X_0 \in \mathcal{X}$

**Output:**  $\hat{X}$

- 1:  $Z_0^{(1)} = Z_0^{(2)} = Z_0^{(3)} \leftarrow X_0$
  - 2: **for**  $k = 0, 1, \dots, K - 1$  **do**
  - 3:  $\bar{Z}_k \leftarrow (Z_k^{(1)} + Z_k^{(2)} + Z_k^{(3)})/3$
  - 4:  $X_{k+1} \leftarrow \mathcal{P}_{\mathcal{X}}(\bar{Z}_k) = \min \left\{ 1, \sqrt{d}/\|\bar{Z}_k\|_F \right\} \cdot \bar{Z}_k$
  - 5:  $Z_{k+1}^{(1)} \leftarrow Z_k^{(1)} - X_{k+1} + \mathbf{prox}_{\alpha f_1}(2X_{k+1} - Z_k^{(1)})$
  - 6:  $Z_{k+1}^{(2)} \leftarrow Z_k^{(2)} - X_{k+1} + \mathbf{prox}_{\alpha f_2}(2X_{k+1} - Z_k^{(2)})$
  - 7:  $Z_{k+1}^{(3)} \leftarrow Z_k^{(3)} - X_{k+1} + \mathbf{prox}_{\alpha f_3}(2X_{k+1} - Z_k^{(3)})$
  - 8: **end for**
  - 9: **return**  $\hat{X} = K^{-1} \sum_{k=1}^K X_k$
- 

condition that  $\mathcal{X} = \mathbb{R}^p$ , and below is our formal proof.

If  $g_i(x) = 0$ , then  $d_{G_i}(x)$  is also zero, so the inequality holds trivially. In what follows we assume that  $g_i(x) > 0$ . By definition,  $d_{G_i}^2(x) = \min_{g_i(y) \leq 0} \|y - x\|^2$ , and the Lagrangian for this constrained optimization problem is  $l(y, \lambda) = \|y - x\|^2 + \lambda g_i(y)$ , with the optimality conditions

$$\begin{aligned} g_i(y_*) &\leq 0, \quad \lambda_* \geq 0, \\ \lambda_* g_i(y_*) &= 0, \end{aligned} \tag{15}$$

$$2(y_* - x) + \lambda_* \partial g_i(y_*) \ni 0. \tag{16}$$

Here  $y_*$  and  $\lambda_*$  are the primal and dual optimal points, respectively. By definition,  $y_* = \mathcal{P}_{G_i}(x)$ , and Assumption 3(a) indicates that  $y_* \in \mathcal{X}$ . Since we have assumed that  $g_i(x) > 0$ , it is easy to see that  $y_* - x \neq \mathbf{0}$ , and hence  $\lambda_* \neq 0$  by (16). Consequently,  $g_i(y_*) = 0$  by (15).

Let  $\nabla g_i(y_*)$  be the subgradient such that  $2(y_* - x) + \lambda_* \nabla g_i(y_*) = \mathbf{0}$ , and then we have  $[\nabla g_i(y_*)]^T(x - y_*) = \|x - y_*\| \cdot \|\nabla g_i(y_*)\|$ . Since  $g_i(x)$  is convex, it holds that

$$g_i(x) \geq g_i(y_*) + [\nabla g_i(y_*)]^T(x - y_*) = \|x - y_*\| \cdot \|\nabla g_i(y_*)\| \geq \rho_i \|x - y_*\|,$$

where the last inequality is from Assumption 3(b). Finally by definition,  $d_{G_i}(x) = \|y_* - x\|$ , so the desired inequality holds.

Next we prove part (a) of the theorem. The proof is similar to that of Proposition 2 of [Kundu et al. \(2018\)](#), but under our generalized settings. Since  $f(x)$  is Lipschitz continuous on  $\mathcal{X}$ , we have  $f(y) - f(x) \leq L\|y - x\|$  for all  $x, y \in \mathcal{X}$ . Set  $y = \mathcal{P}_{\mathcal{K}}(x)$ , and then

$$f_* \leq f(y) \leq f(x) + L\|y - x\| = f(x) + L \cdot d_{\mathcal{K}}(x). \quad (17)$$

On one hand, for  $\mu \geq \gamma L$  and all  $x \in \mathcal{X}$ ,

$$\mathcal{L}(x; \mu) \geq f(x) + \mu h(d_{C_1}(x), \dots, d_{C_l}(x), d_{G_1}(x), \dots, d_{G_m}(x)) \geq f(x) + \frac{\mu}{\gamma} d_{\mathcal{K}}(x) \geq f_*, \quad (18)$$

which indicates that  $\mathcal{L}_* \geq f_*$ . On the other hand,  $d_{C_i}(x) = [g_i(x)]_+ = 0$  for all  $x \in \mathcal{K}$ , so  $\mathcal{L}(x; \mu) = f(x)$  on  $\mathcal{K}$ . Therefore,

$$\mathcal{L}_* = \min_{x \in \mathcal{X}} \mathcal{L}(x; \mu) \leq \min_{x \in \mathcal{K}} \mathcal{L}(x; \mu) = \min_{x \in \mathcal{K}} f(x) = f_*.$$

As a result, we must have  $\mathcal{L}_* = f_*$ .

For part (b), if  $\mu \geq \gamma(L + 1)$ , then

$$f(x_\varepsilon) + \frac{\mu}{\gamma} d_{\mathcal{K}}(x_\varepsilon) \stackrel{(i)}{\leq} \mathcal{L}(x_\varepsilon; \mu) \leq f_* + \varepsilon \stackrel{(ii)}{\leq} f(x_\varepsilon) + L \cdot d_{\mathcal{K}}(x_\varepsilon) + \varepsilon,$$

where (i) is true by (18), and (ii) holds due to (17). Hence we get  $\|x_\varepsilon - y_\varepsilon\| = d_{\mathcal{K}}(x_\varepsilon) \leq \varepsilon$ . Finally, using (17) again yields

$$\mathcal{L}(y_\varepsilon; \mu) = f(y_\varepsilon) \leq f(x_\varepsilon) + L \cdot d_{\mathcal{K}}(x_\varepsilon) \leq \mathcal{L}(x_\varepsilon; \mu) \leq \mathcal{L}_* + \varepsilon.$$

## A.5 Proof of Theorem 2

Define  $U = [0, 1]^p$ ,  $T = \{z \in \mathbb{R}^p : z_1 + \dots + z_p = d\}$ , and  $F = U \cap T$ . Let  $\theta = (\theta_1, \dots, \theta_p)^\top$  be the  $p$  eigenvalues of  $X$ , and then  $X \in \mathcal{F}_1 \Leftrightarrow \theta \in T$ ,  $X \in \mathcal{F}_{2,3} \Leftrightarrow \theta \in U$ , and  $X \in \mathcal{F}^d \Leftrightarrow \theta \in F$ . It is also easy to see that  $d_T(\theta) = d_{\mathcal{F}_1}(X)$ ,  $d_U(\theta) = d_{\mathcal{F}_{2,3}}(X)$ , and  $d_F(\theta) = d_{\mathcal{F}^d}(X)$ , so it suffices to prove the following inequality for any  $z \in \mathbb{R}^p$ :

$$d_F(z) \leq \sqrt{p/(d+1)} \cdot d_T(z) + \sqrt{p} \cdot d_U(z).$$

For any  $x \in \partial F$ , the normal cone of  $F$  at  $x$  is defined by  $N_F(x) = \{y : y^\top(x - x') \geq 0, \forall x' \in F\}$ . Below are three important facts about normal cones:

1. It holds that

$$y \in N_F(x) \Leftrightarrow x \in \arg \max_{x' \in F} y^\top x'. \quad (19)$$

2. For all  $x \in F$ ,  $x = P_F(z)$  if and only if  $z - x \in N_F(x)$ .

3. For all  $x \in F$ ,  $y \in N_F(x)$ , and  $t \geq 0$ ,  $P_F(x + ty) = x$ .

Our final goal is to show that there exist constants  $c_1 > 0$  and  $c_2 > 0$  such that

$$d_F(z) \leq c_1 d_U(z) + c_2 d_T(z) \quad (20)$$

for any  $z \in \mathbb{R}^p$ . Using the second fact about normal cones, we can decompose  $z$  as  $z = x + y$ , where  $x = P_F(z)$  and  $y \in N_F(x)$ . For  $x = (x_1, \dots, x_p)^T \in \partial F$ , we divide it into three blocks with index sets  $I_1$ ,  $I_2$ , and  $I_3$  such that

$$\begin{cases} x_k = 1, & k \in I_1, \\ 0 < x_k < 1, & k \in I_2, \\ x_k = 0, & k \in I_3. \end{cases}$$

For simplicity, we can assume  $I_1 = \{1, \dots, i\}$ ,  $I_2 = \{i+1, \dots, j\}$ , and  $I_3 = \{j+1, \dots, p\}$  without loss of generality. Since  $x \in F \subset T$ , we have  $\sum_{i=1}^p x_i = d > 0$ , so  $I_1$  and  $I_2$  cannot be both empty. Moreover, as long as  $d < p$ ,  $I_2$  and  $I_3$  cannot be both empty. Consequently, there are four situations of the emptiness of the index sets: (1)  $I_1 \neq \emptyset$  and  $I_3 \neq \emptyset$ ; (2)  $I_1 \neq \emptyset$ ,  $I_2 \neq \emptyset$ , and  $I_3 = \emptyset$ ; (3)  $I_1 = \emptyset$ ,  $I_2 \neq \emptyset$ , and  $I_3 \neq \emptyset$ ; and (4)  $I_1 = I_3 = \emptyset$  and  $I_2 \neq \emptyset$ .

Using the same index sets,  $y$  can be accordingly divided into three blocks. By definition (19), it must hold that

$$\min_{k \in I_1} y_k \geq y_{i+1} = \dots = y_j \geq \max_{k \in I_3} y_k.$$

Define  $I_U = \{k \in I_1 : y_k > 0\} \cup \{k \in I_3 : y_k < 0\}$ . If  $I_U \neq \emptyset$ , then  $d_U(z) \geq \sqrt{\sum_{k \in I_U} y_k^2}$ . Moreover,  $T$  is a hyperplane in  $\mathbb{R}^p$  with the normal vector  $n_T = (1/\sqrt{p}, \dots, 1/\sqrt{p})^T$ , so  $d_F(z) = \|y\|$  and  $d_T(z) = \|y\| \cdot |\cos \angle(y, n_T)|$ . We separately discuss the result based on whether  $z \in U$  or  $z \notin U$ .

**The case of  $z \in U$**  In this case  $d_U(z) = 0$ , so we only need to find  $c_2$  such that  $c_2^{-1} \leq \inf_{z \in U} |\cos \angle(y, n_T)|$ . Consider the four situations mentioned above.

(1)  $I_1 \neq \emptyset$  and  $I_3 \neq \emptyset$ . Since  $x + y = z \in [0, 1]^p$ , we have  $y_k \leq 0$  for  $k \in I_1$  and  $y_k \geq 0$  for  $k \in I_3$ , which implies that  $y = \mathbf{0}$ . Therefore, (20) holds trivially for any  $c_2$  since  $d_F(z) = d_T(z) = 0$ .

(2)  $I_1 \neq \emptyset$ ,  $I_2 \neq \emptyset$ , and  $I_3 = \emptyset$ . We have  $\min_{k \in I_1} y_k \geq y_{i+1} = \dots = y_p = c$ . Since  $x + y = z \in [0, 1]^p$ , it is true that  $0 \geq y_k \geq c$  for  $k \in I_1$ . We can assume that  $c \neq 0$ , since otherwise  $y = \mathbf{0}$  and it reduces to the trivial case. Note that  $|\cos \angle(y, n_T)| =$

$|\cos \angle(ty, n_T)|$  for any  $t \neq 0$ , so we can take  $t = 1/c$  to obtain

$$|\cos \angle(ty, n_T)| = \frac{|\sum_{k=1}^p ty_k|}{\sqrt{\sum_{k=1}^p (ty_k)^2} \cdot \sqrt{p}} = \frac{p - i + \sum_{k \in I_1} ty_k}{\sqrt{p - i + \sum_{k \in I_1} (ty_k)^2} \cdot \sqrt{p}} \geq \frac{\sqrt{p - i + \sum_{k \in I_1} ty_k}}{\sqrt{p}}.$$

The inequality holds because  $0 \leq (ty_k)^2 \leq ty_k \leq 1$  for  $k \in I_1$ . Using the fact that  $i < d$ , we immediately get  $|\cos \angle(y, n_T)| = |\cos \angle(ty, n_T)| \geq \sqrt{(p - i)/p} > \sqrt{1 - d/p}$ .

(3)  $I_1 = \emptyset$ ,  $I_2 \neq \emptyset$ , and  $I_3 \neq \emptyset$ . In this case  $y_1 = \dots = y_j = c$ , and  $c \geq y_k \geq 0$  for  $k \in I_3$ . Since  $x$  needs to satisfy the condition  $\sum_{k=1}^p x_k = \sum_{k=1}^j x_k = d$  with  $0 < x_k < 1$  for  $k \leq j$ , we have  $j \geq d + 1$ . Using the similar argument in the second case, we take  $t = 1/c$ , and then

$$|\cos \angle(y, n_T)| = |\cos \angle(ty, n_T)| = \frac{j + \sum_{k \in I_3} ty_k}{\sqrt{j + \sum_{k \in I_3} (ty_k)^2} \cdot \sqrt{p}} \geq \sqrt{j/p} \geq \sqrt{(d + 1)/p}.$$

(4)  $I_1 = I_3 = \emptyset$  and  $I_2 \neq \emptyset$  imply  $y_1 = \dots = y_p = c$  and  $|\cos \angle(y, n_T)| = 1$ . To summarize, for  $z \in U$ , we can choose any  $c_2$  such that  $c_2 \geq \sqrt{p/(d + 1)}$ , assuming  $d \leq (p - 1)/2$ .

**The case of  $z \notin U$**  In this case we assert that  $y \neq \mathbf{0}$ , and then without loss of generality we assume that  $y_k$ 's are in decreasing order. Similar to the discussion above, we consider the four situations based on the emptiness of  $I_1$ ,  $I_2$ , and  $I_3$ .

(1) We have  $\min_{k \in I_1} y_k \geq \max_{k \in I_3} y_k$ . Let  $M = \{k : |y_k| \geq |y_{k'}|, k' \neq k\}$ , and then we find that  $M \cap I_U \neq \emptyset$ . Let  $s$  be any element in  $M \cap I_U$ , and we have  $|y_s|/\|y\| \geq 1/\sqrt{p}$ , indicating that  $d_U(z) \geq \sqrt{\sum_{k \in I_U} y_k^2} \geq |y_s| \geq d_F(z)/\sqrt{p}$ .

(2)  $y_1 \geq \dots \geq y_i \geq y_{i+1} = \dots = y_p = c$ . (a) If  $c \geq 0$ , then  $y_1 > 0$  and  $y_1$  has the largest absolute value. (b) If  $c < 0$  but  $|y_1| > |c|$ , then  $y_1$  must be positive and again it has the largest absolute value. In both cases, we get  $d_U(z) \geq d_F(z)/\sqrt{p}$  based on the argument in (1). (c) If  $c < 0$ ,  $|y_1| \leq |c|$ , and  $y_1 \leq 0$ , then same as point (2) in the case of  $z \in U$ , we have  $|\cos \angle(y, n_T)| \geq \sqrt{1 - d/p}$ . (d) At last, let  $s$  be an index such that  $-c \geq y_1 \geq \dots \geq y_s \geq 0 \geq y_{s+1} \geq \dots \geq y_i \geq y_{i+1} = \dots = y_p = c$ , and denote  $S_1 = \sum_{k=1}^s y_k$ ,  $S_2 = \sum_{k=1}^s y_k^2$ , and  $S_3 = -\sum_{k=s+1}^p y_k$ . Clearly  $\sqrt{S_2} \geq S_1/\sqrt{s}$ . Since  $s \leq i \leq d \leq (p - 1)/2$ , we have  $S_1 < S_3$ . Recall that  $d_U(z) \geq \sqrt{S_2}$ ,  $d_F(z) = \|y\|$ , and



$d_T(z) = |S_3 - S_1|/\sqrt{p}$ , so if  $p \geq 4$  then

$$\begin{aligned} & \sqrt{p} \cdot d_U(z) + \sqrt{\frac{p}{d+1}} \cdot d_T(z) \geq \sqrt{pS_2} + (S_3 - S_1)/\sqrt{d+1} \\ & \geq \left\{ \left( \sqrt{p(d+1)/s} - 1 \right) S_1 + S_3 \right\} / \sqrt{d+1} \geq (S_1 + S_3)/\sqrt{d+1} \\ & \geq \frac{\|y\|}{\sqrt{d+1}} \cdot \frac{p-i + \sum_{k \in I_1} |y_k/c|}{\sqrt{p-i + \sum_{k \in I_1} (y_k/c)^2}} \geq \sqrt{\frac{p-d}{d+1}} \cdot \|y\| \geq d_F(z). \end{aligned}$$

(3)  $y_1 = \dots = y_j = c \geq y_{j+1} \geq \dots \geq y_p$ . In the following two cases, (a)  $c \leq 0$ , and (b)  $c > 0$  but  $|y_p| > c$ , we would get  $d_U(z) \geq d_F(z)/\sqrt{p}$  using the argument in (1). For (c)  $c > 0$ ,  $|y_p| \leq c$ , and  $y_p \geq 0$ , point (3) of the case  $z \in U$  shows that  $|\cos \angle(y, n_T)| \geq \sqrt{(d+1)/p}$ . The remaining possibility is (d)  $c > 0$ ,  $|y_p| \leq c$ , and  $y_p < 0$ . Let  $s$  be an index such that  $y_1 = \dots = y_j = c \geq y_{j+1} \geq \dots \geq y_s \geq 0 \geq y_{s+1} \geq \dots \geq y_p \geq -c$ , and denote  $S_1 = -\sum_{k=s+1}^p y_k$ ,  $S_2 = \sum_{k=s+1}^p y_k^2$ ,  $S_3 = \sum_{k=1}^s y_k$ ,  $S_4 = \sum_{k=1}^s y_k^2$ , and

$$S = \sqrt{pS_2} + |S_3 - S_1|/\sqrt{d+1} \leq \sqrt{p} \cdot d_U(z) + \sqrt{\frac{p}{d+1}} \cdot d_T(z).$$

We can assume that  $S_2 \leq \|y\|^2/p$ , since otherwise we directly get  $d_U(z) \geq \sqrt{S_2} > \|y\|/\sqrt{p} = d_F(z)/\sqrt{p}$ . Using the fact that  $s \geq j \geq d+1$ , we have  $S_1 \leq \sqrt{(p-s)S_2} \leq \sqrt{1 - (d+1)/p} \cdot \|y\|$ . On the other hand,  $S_3 \geq \sqrt{S_4} = \sqrt{\|y\|^2 - S_2} \geq \sqrt{1 - 1/p} \cdot \|y\| > S_1$ , so

$$\sqrt{d+1} \cdot S = \sqrt{p(d+1)S_2} - S_1 + S_3 \geq \left( \sqrt{\frac{p(d+1)}{p-s}} - 1 \right) S_1 + S_3 \geq S_1 + S_3$$

as long as  $d \geq 3$ . Note that

$$\frac{S_1 + S_3}{\|y\|} = \frac{\sum_{k=1}^p |y_k|}{\sqrt{\sum_{k=1}^p y_k^2}} = \frac{j + \sum_{k=j+1}^p |ty_k|}{\sqrt{j + \sum_{k=j+1}^p (ty_k)^2}} \geq \sqrt{j + \sum_{k=j+1}^p |ty_k|} \geq \sqrt{d+1}$$

for  $t = 1/c$ , and we finally get  $S \geq \|y\| = d_F(z)$ .

(4) The last case  $I_1 = I_3 = \emptyset$  is trivial, which completes the proof.

## A.6 Proof of Corollary 1

First, since

$$\begin{aligned}
|f(X) - f(Y)| &= |\operatorname{tr}(S(Y - X)) + \lambda(\|X\|_{1,1} - \|Y\|_{1,1})| \\
&\leq |\operatorname{tr}(S(Y - X))| + \lambda|\|X\|_{1,1} - \|Y\|_{1,1}| \\
&\leq \|S\|_F \cdot \|X - Y\|_F + \lambda\|X - Y\|_{1,1} \\
&\leq \|S\|_F \cdot \|X - Y\|_F + \lambda p\|X - Y\|_F,
\end{aligned}$$

we find that  $f(X)$  is Lipschitz continuous with  $L = \|S\|_F + \lambda p$ .

Second, part (a) of the assumption is trivial. For part (b), recall that  $g_2(X) = -\theta_p(X)$ . Appendix F of [Yang et al. \(2017\)](#) shows that for any  $Y \in \bar{G}_2$ ,  $\|\nabla g_2(Y)\|_F \geq 1/\sqrt{s_0}$ , where  $\nabla g_2(Y)$  is any subgradient of  $g_2$  at  $Y$ , and  $s_0$  is the number of zero eigenvalues of  $Y$ . Obviously  $s_0 \leq p$ , so we get  $\rho_2 = 1/\sqrt{p}$ . Note that  $g_1(X) = \theta_1(X) - 1 = g_2(I - X)$ . Using the same argument,  $\rho_1 \geq 1/\sqrt{s_1}$ , where  $s_1$  is the number of eigenvalues equal to one for a matrix  $Y \in \bar{G}_1 \cap \mathcal{X}$ . Since  $Y \in \mathcal{X} \Rightarrow \|Y\|_F \leq \sqrt{d}$ , we have  $s_1 \leq d$ , so we can take  $\rho_1 = 1/\sqrt{d}$ .

Third, it is not hard to show that  $d_{\mathcal{F}_{2,3}}(X) = \sqrt{[d_{G_1}(X)]^2 + [d_{G_2}(X)]^2} \leq d_{G_1}(X) + d_{G_2}(X)$ . Then Theorem 2 gives the desired result.

## A.7 Proof of Theorem 3

The proof mainly follows from [Ryu and Yin \(2017\)](#), and our new result is to give explicit constants instead of the mere rate of convergence in [Ryu and Yin \(2017\)](#). For completeness we include the main steps of the proof here. We use the notation  $\mathbf{X} = (X^{(1)}, X^{(2)})$  to denote a collection of two  $p \times p$  matrices, and then define the functions  $r(\mathbf{X}) = I_{\mathcal{E}}(\mathbf{X})$  and  $g(\mathbf{X}) = f_1(X^{(1)}) + f_2(X^{(2)})$ , where  $I_{\mathcal{E}}(\mathbf{X}) = 0$  if  $X^{(1)} = X^{(2)} \in \mathcal{X}$ , and  $I_{\mathcal{E}}(\mathbf{X}) = \infty$  otherwise. Since  $f_1$  and  $f_2$  are Lipschitz continuous with constants  $L_1 = \lambda p$  and  $L_2 = \|S\|_F + \mu(1 + \sqrt{(p+d)(d+1)})$ , respectively, it is easy to show that

$$\begin{aligned}
|g(\mathbf{X}) - g(\mathbf{Y})| &\leq |f_1(X^{(1)}) - f_1(Y^{(1)})| + |f_2(X^{(2)}) - f_2(Y^{(2)})| \\
&\leq L_1\|X^{(1)} - Y^{(1)}\|_F + L_2\|X^{(2)} - Y^{(2)}\|_F \\
&\leq \sqrt{L_1^2 + L_2^2} \cdot \sqrt{\|X^{(1)} - Y^{(1)}\|_F^2 + \|X^{(2)} - Y^{(2)}\|_F^2} \\
&= \sqrt{L_1^2 + L_2^2} \cdot \|\mathbf{X} - \mathbf{Y}\|_F.
\end{aligned}$$

Therefore,  $g(\cdot)$  is Lipschitz continuous with the constant  $L_g = \sqrt{L_1^2 + L_2^2}$ .

Denote  $\mathbf{X}_k = (X_k, X_k)$ ,  $\mathbf{Z}_k = (Z_k^{(1)}, Z_k^{(2)})$ , and then Algorithm 1 can be equivalently

expressed as

$$\mathbf{X}_{k+1} = \mathbf{prox}_{\alpha r}(\mathbf{Z}_k), \quad (21)$$

$$\mathbf{Y}_{k+1} = \mathbf{prox}_{\alpha g}(2\mathbf{X}_{k+1} - \mathbf{Z}_k), \quad (22)$$

$$\mathbf{Z}_{k+1} = \mathbf{Z}_k - \mathbf{X}_{k+1} + \mathbf{Y}_{k+1}.$$

Define the function  $p(\mathbf{Z}) = (1/\alpha)(\mathbf{X} - \mathbf{Y})$ , where  $\mathbf{X} = \mathbf{prox}_{\alpha r}(\mathbf{Z})$  and  $\mathbf{Y} = \mathbf{prox}_{\alpha g}(2\mathbf{X} - \mathbf{Z})$ , so we have  $p(\mathbf{Z}_k) = (1/\alpha)(\mathbf{X}_{k+1} - \mathbf{Y}_{k+1})$  and  $\mathbf{Z}_{k+1} = \mathbf{Z}_k - \alpha p(\mathbf{Z}_k)$ . Let  $X_* \in \arg \min_{X \in \mathcal{X}} \mathcal{L}(X)$  and denote  $\mathbf{X}_* = (X_*, X_*)$ . Then we have  $\mathbf{X}_* \in \arg \min_{\mathbf{X}} r(\mathbf{X}) + g(\mathbf{X})$ , whose optimality condition indicates that  $\nabla r(\mathbf{X}_*) + \nabla g(\mathbf{X}_*) = \mathbf{O}$ , where  $\nabla r(\cdot)$  and  $\nabla g(\cdot)$  are some specific subgradients of  $r(\cdot)$  and  $g(\cdot)$ , respectively. Clearly we have  $\|\nabla g(\mathbf{X}_*)\|_F = \|\nabla r(\mathbf{X}_*)\|_F \leq L_g$ . Moreover, Lemma 1 of [Ryu and Yin \(2017\)](#) shows that there exists  $\mathbf{Z}_* = (Z_*^{(1)}, Z_*^{(2)})$  such that  $p(\mathbf{Z}_*) = \mathbf{O}$  and  $\mathbf{X}_* = \mathbf{prox}_{\alpha r}(\mathbf{Z}_*)$ .

Next, Lemma 4 of [Ryu and Yin \(2017\)](#) proves that  $\alpha\|p(\mathbf{Z}) - p(\mathbf{Z}')\|_F^2 \leq \langle p(\mathbf{Z}) - p(\mathbf{Z}'), \mathbf{Z} - \mathbf{Z}' \rangle$  for any  $\mathbf{Z}$  and  $\mathbf{Z}'$ , where  $\langle \mathbf{X}, \mathbf{Y} \rangle = \text{vec}(\mathbf{X})^T \text{vec}(\mathbf{Y})$ . Therefore,

$$\begin{aligned} \|p(\mathbf{Z}_{k+1})\|_F^2 &= \|p(\mathbf{Z}_k)\|_F^2 + 2\langle p(\mathbf{Z}_{k+1}) - p(\mathbf{Z}_k), p(\mathbf{Z}_k) \rangle + \|p(\mathbf{Z}_{k+1}) - p(\mathbf{Z}_k)\|_F^2 \\ &= \|p(\mathbf{Z}_k)\|_F^2 - 2\alpha^{-1}\langle p(\mathbf{Z}_{k+1}) - p(\mathbf{Z}_k), \mathbf{Z}_{k+1} - \mathbf{Z}_k \rangle + \|p(\mathbf{Z}_{k+1}) - p(\mathbf{Z}_k)\|_F^2 \\ &\leq \|p(\mathbf{Z}_k)\|_F^2 - \|p(\mathbf{Z}_{k+1}) - p(\mathbf{Z}_k)\|_F^2, \end{aligned}$$

for any  $k \geq 0$ , implying that  $\|p(\mathbf{Z}_k)\|_F^2$  is monotonically decreasing. Using the inequality again, we have  $\alpha\|p(\mathbf{Z}_k) - p(\mathbf{Z}_*)\|_F^2 = \alpha\|p(\mathbf{Z}_k)\|_F^2 \leq \langle p(\mathbf{Z}_k) - p(\mathbf{Z}_*), \mathbf{Z}_k - \mathbf{Z}_* \rangle = \langle p(\mathbf{Z}_k), \mathbf{Z}_k - \mathbf{Z}_* \rangle$ , so

$$\begin{aligned} \|\mathbf{Z}_{k+1} - \mathbf{Z}_*\|_F^2 &= \|\mathbf{Z}_k - \mathbf{Z}_*\|_F^2 - 2\alpha\langle p(\mathbf{Z}_k), \mathbf{Z}_k - \mathbf{Z}_* \rangle + \alpha^2\|p(\mathbf{Z}_k)\|_F^2 \\ &\leq \|\mathbf{Z}_k - \mathbf{Z}_*\|_F^2 - \alpha^2\|p(\mathbf{Z}_k)\|_F^2, \end{aligned}$$

showing that  $\|\mathbf{Z}_k - \mathbf{Z}_*\|_F^2$  is also monotone. Define  $C_0 = \|\mathbf{Z}_0 - \mathbf{Z}_*\|_F$ , and then  $\|\mathbf{Z}_k - \mathbf{Z}_*\|_F^2 \leq C_0^2$  and  $\|\mathbf{Z}_k - \mathbf{Z}_s\|_F \leq 2C_0$  for all  $k, s \geq 0$ . Consequently,

$$\sum_{k=0}^{\infty} \|p(\mathbf{Z}_k)\|_F^2 \leq \frac{1}{\alpha^2} \|\mathbf{Z}_0 - \mathbf{Z}_*\|_F^2 = \frac{C_0^2}{\alpha^2}, \quad (23)$$

$$\|p(\mathbf{Z}_k)\|_F^2 \leq \frac{1}{k} \sum_{k=0}^{\infty} \|p(\mathbf{Z}_k)\|_F^2 \leq \frac{C_0^2}{k\alpha^2}, \quad (24)$$

where (24) is due to the monotonicity of  $\|p(\mathbf{Z}_k)\|_F^2$ .

Define  $\bar{\mathbf{X}}_k = k^{-1} \sum_{j=1}^k \mathbf{X}_j$ ,  $\bar{\mathbf{Y}}_k = k^{-1} \sum_{j=1}^k \mathbf{Y}_j$ , and  $\bar{E}_k = g(\bar{\mathbf{Y}}_k) - g(\mathbf{X}_*)$ . Equations

(29), (31), and (34) of [Ryu and Yin \(2017\)](#) show that

$$\begin{aligned}\frac{1}{2}\bar{E}_k &\leq \frac{1}{2\alpha k}\|\mathbf{Z}_1 - \mathbf{Z}_*\|_F^2 + \frac{1}{k\alpha}\|\mathbf{Z}_{k+1} - \mathbf{Z}_1\|_F \cdot \|\nabla r(\mathbf{X}_*)\|_F, \\ \frac{1}{2}\bar{E}_k &\geq \frac{1}{k}\langle \mathbf{Z}_k - \mathbf{Z}_0, \nabla r(\mathbf{X}_*) \rangle \geq -\frac{1}{k}\|\mathbf{Z}_k - \mathbf{Z}_0\|_F \cdot \|\nabla r(\mathbf{X}_*)\|_F,\end{aligned}$$

and then by bounding the relevant terms we get  $|\bar{E}_k| \leq \max\{(C_0^2 + 4C_0L_g)/(\alpha k), 2C_0L_g/k\}$ . Moreover,

$$|g(\bar{\mathbf{X}}_k) - g(\bar{\mathbf{Y}}_k)| \leq L_g\|\bar{\mathbf{X}}_k - \bar{\mathbf{Y}}_k\|_F = (L_g/k)\|\mathbf{Z}_{k+1} - \mathbf{Z}_k\|_F \leq 2C_0L_g/k,$$

and then  $|g(\bar{\mathbf{X}}_k) - g(\mathbf{X}_*)| \leq |\bar{E}_k| + 2C_0L_g/k$ , implying the first result. The second result is a consequence of [Theorem 1\(b\)](#).

## A.8 Proof of [Corollary 2](#)

Denote  $\mathcal{L}_* = \min_{X \in \mathcal{X}} \mathcal{L}(X) = \mathcal{L}(\hat{X}_*)$  and let  $\hat{Y} = \mathcal{P}_{\mathcal{K}}(\hat{X})$ . [Theorem 3](#) shows that  $\|\hat{Y} - \hat{X}\|_F \leq C/T$  and  $\mathcal{L}(\hat{X}) \leq \mathcal{L}_* + C/T$ . Also [Theorem 1\(b\)](#) indicates that  $\mathcal{L}(\hat{Y}) = f(\hat{Y}) \leq \mathcal{L}_* + C/T \leq f(\Pi) + C/T$ .

Let  $\Delta = \hat{Y} - \Pi$  and  $W = S - \Sigma$ , and then [Lemma 3.1](#) of [Vu et al. \(2013\)](#) implies that  $(\delta/2)\|\Delta\|_F^2 \leq -\text{tr}(\Sigma\Delta)$ . Therefore, if  $\lambda \geq \|W\|_{\infty, \infty}$ , then

$$\begin{aligned}(\delta/2)\|\Delta\|_F^2 &\leq -\text{tr}(\Sigma\Delta) = -\text{tr}(S\Delta) + \text{tr}(W\Delta) \\ &= f(\hat{Y}) - f(\Pi) - \lambda(\|\hat{Y}\|_{1,1} - \|\Pi\|_{1,1}) + \text{tr}(W\Delta) \\ &\leq_{(*)} f(\hat{Y}) - f(\Pi) + 2\lambda s\|\Delta\|_F \\ &\leq 2\lambda s\|\Delta\|_F + C/T,\end{aligned}$$

where  $(*)$  comes from the proof of [Theorem 3.1](#) of [Vu et al. \(2013\)](#). Solving the inequality above, we get

$$\|\Delta\|_F \leq \frac{2\lambda s + \sqrt{(2\lambda s)^2 + 2\delta C/T}}{\delta} \leq \frac{4\lambda s}{\delta} + \frac{\sqrt{2C/\delta}}{\sqrt{T}},$$

and hence  $\|\hat{X} - \Pi\|_F \leq \|\Delta\|_F + \|\hat{X} - \hat{Y}\|_F \leq \|\Delta\|_F + C/T$ . Under the stated assumptions,  $\|W\|_{\infty, \infty} \leq \lambda$  holds with probability at least  $1 - 2/p^2$ , thus proving the conclusion.

## A.9 Proof of [Theorem 4 \(Part One\)](#)

Define  $f_{0t}(X) = -\text{tr}(S_t X)$ ,  $f_1(X) = \lambda\|X\|_1$ ,  $f_2(X) = \nu\sqrt{pd}[g_1(X)]_+ + \nu p[g_2(X)]_+$ , and  $f_3(X) = \nu\sqrt{p/(d+1)}d_{C_1}(X)$ . Then by [Corollary 1](#),  $\nu d_{\mathcal{K}}(X) \leq f_2(X) + f_3(X)$ , so we get  $\ell_{t-1}(X) \leq (f_{0t} + f_1 + f_2 + f_3)(X)$ . Moreover,  $\ell_{t-1}(X) = f_{0t}(X) + f_1(X)$  if  $X \in \mathcal{K}$ . Below we first follow [Proposition 3](#) of [Bertsekas \(2011\)](#) to obtain inequalities [\(25\)](#) to

(32), and then adapt the results to the online learning setting.

It is easy to see that  $X_t^{(1)} = \mathbf{prox}_{\alpha_t f_1}(X_t^{(0)})$  and  $X_t^{(3)} = \mathbf{prox}_{\alpha_t f_3}(X_t^{(2)})$ , so by Proposition 1(b) of Bertsekas (2011), for any  $Y \in \mathcal{X}$  we have

$$f_1(X_t^{(1)}) - f_1(Y) \leq \frac{1}{2\alpha_t} \left( \|X_t^{(0)} - Y\|_F^2 - \|X_t^{(1)} - Y\|_F^2 \right), \quad (25)$$

$$f_3(X_t^{(3)}) - f_3(Y) \leq \frac{1}{2\alpha_t} \left( \|X_t^{(2)} - Y\|_F^2 - \|X_t^{(3)} - Y\|_F^2 \right). \quad (26)$$

Next, the convexity of  $f_2$  implies  $f_2(X_t^{(1)}) - f_2(Y) \leq \text{tr}(G(X_t^{(1)} - Y))$ , where  $G$  is any subgradient of  $f_2$  at  $X_t^{(1)}$ . Take  $G = \alpha_t \nu \sqrt{pd} \mathbf{1}\{\lambda_1 > 1\} \gamma_1 \gamma_1^T - \alpha_t \nu p \mathbf{1}\{\lambda_p < 0\} \gamma_p \gamma_p^T$ , and then we get

$$\begin{aligned} \|X_t^{(2)} - Y\|_F^2 &= \|X_t^{(1)} - \alpha_t G - Y\|_F^2 = \|X_t^{(1)} - Y\|_F^2 - 2\alpha_t \text{tr}(G(X_t^{(1)} - Y)) + \alpha_t^2 \|G\|_F^2 \\ &\leq \|X_t^{(1)} - Y\|_F^2 - 2\alpha_t \{f_2(X_t^{(1)}) - f_2(Y)\} + \alpha_t^2 \nu^2 p(p+d), \end{aligned}$$

indicating that

$$f_2(X_t^{(1)}) - f_2(Y) \leq \frac{1}{2\alpha_t} \left( \|X_t^{(1)} - Y\|_F^2 - \|X_t^{(2)} - Y\|_F^2 \right) + \frac{\alpha_t}{2} \nu^2 p(p+d). \quad (27)$$

For  $f_{0t}$ , we have

$$\begin{aligned} \|X_t - Y\|_F^2 &= \|\mathcal{P}_{\mathcal{X}}(X_t^{(3)} + \alpha_t S_t) - Y\|_F^2 \\ &\leq \|X_t^{(3)} + \alpha_t S_t - Y\|_F^2 = \|X_t^{(3)} - Y\|_F^2 - 2\alpha_t \{f_{0t}(X_t^{(3)}) - f_{0t}(Y)\} + \alpha_t^2 \|S_t\|_F^2 \end{aligned}$$

where the inequality is due to the nonexpansion property of the projection operator. As a result,

$$f_{0t}(X_t^{(3)}) - f_{0t}(Y) \leq \frac{1}{2\alpha_t} \left( \|X_t^{(3)} - Y\|_F^2 - \|X_t - Y\|_F^2 \right) + \frac{\alpha_t}{2} \|S_t\|_F^2. \quad (28)$$

Notice that  $f_{0t}$ ,  $f_1$ ,  $f_2$ , and  $f_3$  are all Lipschitz continuous functions, so  $\|X_t^{(1)} - X_t^{(0)}\| \leq \alpha_t \lambda p$ ,  $\|X_t^{(2)} - X_t^{(1)}\| \leq \alpha_t \nu \sqrt{p(p+d)}$ , and  $\|X_t^{(3)} - X_t^{(2)}\| \leq \alpha_t \nu \sqrt{p/(d+1)}$ . Consequently,

$$f_1(X_t^{(0)}) - f_1(X_t^{(1)}) \leq \alpha_t (\lambda p)^2, \quad (29)$$

$$f_2(X_t^{(0)}) - f_2(X_t^{(1)}) \leq \alpha_t \lambda p \nu \sqrt{p(p+d)}, \quad (30)$$

$$f_3(X_t^{(0)}) - f_3(X_t^{(3)}) \leq \alpha_t \nu \sqrt{p/(d+1)} (\lambda p + \nu \sqrt{p(p+d)} + \nu \sqrt{p/(d+1)}), \quad (31)$$

$$f_{0t}(X_t^{(0)}) - f_{0t}(X_t^{(3)}) \leq \alpha_t \|S_t\|_F (\lambda p + \nu \sqrt{p(p+d)} + \nu \sqrt{p/(d+1)}). \quad (32)$$

Adding up (25) to (32), we obtain

$$\ell_{t-1}(X_{t-1}) - \ell_{t-1}(Y) \leq \frac{\|X_{t-1} - Y\|_F^2 - \|X_t - Y\|_F^2}{2\alpha_t} + \frac{\alpha_t}{2} (\|S_t\|_F^2 + C_1 \|S_t\|_F + C_2), \quad (33)$$

where  $C_1 = \lambda p + \nu \sqrt{p(p+d)} + \nu \sqrt{p/(d+1)}$  and  $C_2 = \nu^2 p(p+d) + 2(\lambda p)^2 + 2\lambda p \nu \sqrt{p(p+d)} + 2\nu \sqrt{p/(d+1)} C_1$ . Summarizing (33) over  $t = 2, \dots, T+1$ , we have

$$\begin{aligned} & \sum_{t=1}^T \ell_t(X_t) - \sum_{t=1}^T \ell_t(Y) \\ & \leq \frac{\|X_1 - Y\|_F^2}{2\alpha_2} + \frac{1}{2} \sum_{t=2}^T (\alpha_{t+1}^{-1} - \alpha_t^{-1}) \|X_t - Y\|_F^2 + \frac{1}{2} \sum_{t=2}^{T+1} \alpha_t (\|S_t\|_F^2 + C_1 \|S_t\|_F) + \frac{C_2}{2} \sum_{t=2}^{T+1} \alpha_t \\ & \leq \frac{2d}{\alpha_2} + 2d \cdot \sum_{t=2}^T (\alpha_{t+1}^{-1} - \alpha_t^{-1}) + \frac{C_2}{2} \sum_{t=2}^{T+1} \alpha_t + \frac{1}{2} \sum_{t=2}^{T+1} \alpha_t (\|S_t\|_F^2 + C_1 \|S_t\|_F). \end{aligned}$$

Take  $\alpha_1 = \alpha_0$ ,  $\alpha_t = \alpha_0 / \sqrt{t-1}$ ,  $t \geq 2$ , and then  $\sum_{t=2}^{T+1} \alpha_t \leq 2\alpha_0 \sqrt{T}$  and

$$\sum_{t=1}^T \ell_t(X_t) - \sum_{t=1}^T \ell_t(Y) \leq \frac{2d}{\alpha_0} + \frac{2d\sqrt{T}}{\alpha_0} - \frac{2d}{\alpha_0} + \alpha_0 C_2 \sqrt{T} + \frac{\alpha_0}{2} \sum_{t=1}^T \frac{\|S_{t+1}\|_F^2 + C_1 \|S_{t+1}\|_F}{\sqrt{t}}. \quad (34)$$

## A.10 Proof of Theorem 4 (Part Two)

Let  $f_0(X) = -\text{tr}(\Sigma X)$  and  $\ell = f_0 + f_1 + f_2 + f_3$ , and then it is easy to show that

$$\sum_{t=1}^T \{\ell(X_t) - \ell_t(X_t)\} - \sum_{t=1}^T \{\ell(\Pi) - \ell_t(\Pi)\} = \sum_{t=1}^T \text{tr}((S_{t+1} - \Sigma)(X_t - \Pi)) := \sum_{t=1}^T \eta_t. \quad (35)$$

Combining (34) and (35) yields

$$\frac{1}{T} \sum_{t=1}^T \ell(X_t) - \ell(\Pi) \leq \frac{2d/\alpha_0 + \alpha_0 C_2}{\sqrt{T}} + \frac{\alpha_0}{2T} \sum_{t=1}^T \frac{\|S_{t+1}\|_F^2 + C_1 \|S_{t+1}\|_F}{\sqrt{t}} + \frac{1}{T} \sum_{t=1}^T \eta_t,$$

so our target is to bound  $\sum_{t=1}^T \eta_t$ ,  $\sum_{t=1}^T \|S_{t+1}\|_F / \sqrt{t}$ , and  $\sum_{t=1}^T \|S_{t+1}\|_F^2 / \sqrt{t}$ .

First, note that  $\eta_t \leq \|S_{t+1} - \Sigma\|_F \|X_t - \Pi\|_F \leq 2\sqrt{d}\xi_{t+1}$ , so by Assumption 6,

$$E\{\exp(u\eta_t)\} \leq E\{\exp(2\sqrt{d}u\xi_{t+1})\} \leq \exp(4du^2\sigma_1^2/2), \quad \forall |u| \leq 1/b_1.$$

Also note that  $\eta_t$  is a martingale difference sequence, so

$$\begin{aligned} & E\left\{\exp\left(u\sum_{t=1}^T \eta_t\right)\right\} = E\left\{\exp\left(u\sum_{t=1}^T \eta_t\right) E[\exp(u\eta_T) | S_1, \dots, S_T]\right\} \\ & \leq \exp(4du^2\sigma_1^2/2) \cdot E\left\{\exp\left(u\sum_{t=1}^{T-1} \eta_t\right)\right\} \leq \dots \leq \exp(4d\sigma_1^2 T u^2/2), \end{aligned}$$

showing that  $\sum_{t=1}^T \eta_t$  is sub-exponential with parameters  $b_T = b_1$  and  $\sigma_{1T} = 2\sigma_1 \sqrt{dT}$ .

Using the concentration bound for sub-exponential random variables, we have for any

$D_1 > 0$ ,

$$\begin{aligned} \log \left[ P \left\{ \sum_{t=1}^T \eta_t > D_1 \sqrt{T} \right\} \right] &\leq \begin{cases} -D_1^2/(8\sigma_1^2 d), & D_1 \sqrt{T} \leq \sigma_{1T}^2/b_1 \\ -D_1 \sqrt{T}/(2b_1), & D_1 \sqrt{T} > \sigma_{1T}^2/b_1 \end{cases} \\ &\leq -\min \{ D_1^2/(8\sigma_1^2 d), D_1/(2b_1) \}, \end{aligned} \quad (36)$$

where the conservative bound (36) is used mainly for brevity.

On the other hand,

$$\sum_{t=1}^T \frac{\|S_{t+1}\|_F}{\sqrt{t}} \leq \sum_{t=1}^T \frac{\|S_{t+1} - \Sigma\|_F + \|\Sigma\|_F}{\sqrt{t}} \leq \sum_{t=1}^T \frac{\xi_{t+1} - \mu_1}{\sqrt{t}} + 2\sqrt{T}(\mu_1 + \|\Sigma\|_F).$$

Since  $\xi_t$  is an independent and sub-exponential sequence, we have for all  $|\lambda| < 1/b_1$ ,

$$\begin{aligned} E \left\{ \exp \left( u \sum_{t=1}^T \frac{\xi_{t+1} - \mu_1}{\sqrt{t}} \right) \right\} &= \prod_{t=1}^T E \left[ \exp \left\{ \frac{u(\xi_{t+1} - \mu_1)}{\sqrt{t}} \right\} \right] \\ &\leq \prod_{t=1}^T \exp \left( \frac{u^2 \sigma_1^2}{2t} \right) \leq \exp \{ u^2 \sigma_1^2 (\log(T) + 1)/2 \}. \end{aligned}$$

Therefore, for any  $D_2 > 0$ ,

$$\begin{aligned} \log \left[ P \left\{ \sum_{t=1}^T \frac{\xi_{t+1} - \mu_1}{\sqrt{t}} > D_2 \ell(T) \right\} \right] &\leq \begin{cases} -D_2^2/(2\sigma_1^2), & D_2 \ell(T) \leq \sigma_{2T}^2/b_1 \\ -D_2 \ell(T)/(2b_1), & D_2 \ell(T) > \sigma_{2T}^2/b_1 \end{cases} \\ &\leq -\min \{ D_2^2/(2\sigma_1^2), D_2/(2b_1) \}, \end{aligned} \quad (37)$$

where  $\ell(T) = \sqrt{\log(T) + 1}$ , and  $\sigma_{2T} = \sigma_1 \ell(T)$ . With a similar argument, we can show that  $\sum_{t=1}^T \|S_{t+1}\|_F^2/\sqrt{t} \leq 2\sqrt{T}\mu_2 + \sum_{t=1}^T (\zeta_{t+1} - \mu_2)/\sqrt{t}$ , and for any  $D_3 > 0$ ,

$$\log \left[ P \left\{ \sum_{t=1}^T \frac{\zeta_{t+1} - \mu_2}{\sqrt{t}} > D_3 \ell(T) \right\} \right] \leq -\min \{ D_3^2/(2\sigma_2^2), D_3/(2b_2) \}. \quad (38)$$

Let the right hand sides of (36) (37) (38) be  $\varepsilon/3$ , and we solve  $D_1 = \max \{ 2b_1\varepsilon_l, 2\sigma_1\sqrt{2d\varepsilon_l} \}$ ,  $D_2 = \max \{ 2b_1\varepsilon_l, \sigma_1\sqrt{2\varepsilon_l} \}$ , and  $D_3 = \max \{ 2b_2\varepsilon_l, \sigma_2\sqrt{2\varepsilon_l} \}$ , where  $\varepsilon_l = \log(3/\varepsilon)$ . Therefore, with probability at least  $1 - \varepsilon$ ,

$$\begin{aligned} \frac{1}{T} \mathcal{R}(\{X_t\}, T) &\leq \frac{2d/\alpha_0 + \alpha_0 C_2 + D_1}{\sqrt{T}} + \frac{\alpha_0 C_1 \{ 2\sqrt{T}(\mu_1 + \|\Sigma\|_F) + D_2 \ell(T) \}}{2T} \\ &\quad + \frac{\alpha_0 \{ 2\sqrt{T}\mu_2 + D_3 \ell(T) \}}{2T} \\ &= \frac{C_3}{\sqrt{T}} + \frac{C_4 \{ \log(T) + 1 \}}{T} := C(T), \end{aligned}$$



where  $C_3 = 2d/\alpha_0 + D_1 + \alpha_0\{C_2 + C_1(\mu_1 + \|\Sigma\|_F) + \mu_2\}$ , and  $C_4 = \alpha_0(C_1D_2 + D_3)/2$ . By the convexity of  $\ell(\cdot)$ , we have  $T^{-1} \sum_{t=1}^T \ell(X_t) \geq \ell(\hat{X}_T)$ , so with the specified probability,  $\ell(\hat{X}_T) - \ell(\Pi) \leq C(T)$ .

Let  $\hat{Y}_T = \mathcal{P}_{\mathcal{K}}(\hat{X}_T)$ . If  $\nu \geq \lambda p + \|\Sigma\|_F + 1$ , then by Theorem 1, we have  $\ell(\hat{Y}_T) - \ell(\Pi) \leq C(T)$  and  $\|\hat{X}_T - \hat{Y}_T\| \leq C(T)$ . Let  $\Delta = \hat{Y}_T - \Pi$ , and then Lemma 3.1 of [Vu et al. \(2013\)](#) shows that  $(\delta/2)\|\Delta\|_F^2 \leq -\text{tr}(\Sigma\Delta)$ , thus  $(\delta/2)\|\Delta\|_F^2 \leq -\text{tr}(\Sigma\Delta) = \ell(\hat{Y}_T) - \ell(\Pi) - \lambda(\|\hat{X}_T\|_{1,1} - \|\Pi\|_{1,1}) \leq C(T) + \lambda\|\Pi\|_{1,1}$ . Since  $\Pi$  is sparse, we have  $\|\Pi\|_{1,1} \leq s\|\Pi\|_F = s\sqrt{d}$ . Finally, applying the triangle inequality yields the requested result.

## A.11 Proof of Theorem 5

To simplify the notation, in this proof we use  $\|\cdot\|_q$  as a shorthand for the  $\|\cdot\|_{q,q}$  norm, and let  $\mathbb{S}^p$  be the space of  $p \times p$  symmetric matrices. We first show that the function  $\rho(X) = \|X\|_r^2/2$  is  $\beta$ -strongly convex with respect to the  $\|\cdot\|_1$  norm. To see this, by Lemma 9 of [Kakade et al. \(2012\)](#), we have  $\rho(X) \geq \rho(Y) + \text{tr}(U(X - Y)) + \{(r - 1)/2\}\|X - Y\|_r^2$  for all  $X, Y \in \mathbb{S}^p$  and  $U \in \partial\rho(Y)$ . In general, for  $0 < m < n$  we have  $\|X\|_m \leq p^{2/m-2/n}\|X\|_n$ , so  $\|X\|_1 \leq p^{2-2/r}\|X\|_r = \exp(2)\|X\|_r$ . Then we immediately get  $\rho(X) \geq \rho(Y) + \text{tr}(U(X - Y)) + (\beta/2)\|X - Y\|_1^2$ .

Next we verify that  $f(X; Y, t) = -\text{tr}(YX) + \lambda t\|X\|_1 + \sqrt{t}\|X\|_r^2/2$  is Lipschitz continuous on  $\mathcal{X}$  with the Lipschitz constant  $L_t$ . It is easy to show that the first two terms have Lipschitz constants  $\|Y\|_F$  and  $\lambda tp$ , respectively. For the third term,

$$\frac{\partial(\|X\|_r^2/2)}{\partial x_{kl}} = \frac{1}{r} \left( \sum_{i,j} |x_{ij}|^r \right)^{2/r-1} r |x_{kl}|^{r-1} \text{sign}(x_{kl}), \quad (39)$$

implying that  $\|\nabla\rho(X)\|_F = \|X\|_r^{2-r} \cdot \|X\|_{2r-2}^{r-1} \leq \exp(-4)p^2 \cdot \|X\|_F$ . So the Lipschitz constant for the third term is  $\exp(-4)\sqrt{td}p^2$ . Adding the constants together yields the required result.

Using the notation in [Orabona et al. \(2015\)](#), define  $F(X) = \lambda\|X\|_1$ ,  $g(X) = \rho(X) = \|X\|_r^2/2$ , and  $f_t(X) = \sqrt{t}g(X) + tF(X)$ . The domain of  $f_t(X)$  is taken to be  $\mathcal{K}$ . From the first result above, it is obvious that  $f_t(X)$  is  $\beta\sqrt{t}$ -strongly convex with respect to  $\|\cdot\|_1$ . Let  $f_t^*(Y) = \sup_{X \in \mathcal{K}} \{\text{tr}(YX) - f_t(X)\}$  be the Fenchel conjugate of  $f_t$ , with  $\mathbb{S}^p$  as the domain. [Orabona et al. \(2015\)](#) shows that  $f_t^*$  is everywhere differentiable, and  $\nabla f_t^*(Y) = \arg \min_{X \in \mathcal{K}} \{-\text{tr}(YX) + f_t(X)\}$ .

Let  $W_t = \nabla f_t^*(Y_t) = \arg \min_{X \in \mathcal{K}} \{-\text{tr}(Y_t X) + f_t(X)\}$ , and then Theorem 1(a) indicates that  $\mathring{\mathcal{L}}_* := \min_{X \in \mathcal{X}} \mathring{\mathcal{L}}(X; Y_t, t) = \mathring{\mathcal{L}}(W_t; Y_t, t)$ . Also let  $X_t$  be defined as in

Algorithm 3, so by definition,  $\mathring{\mathcal{L}}(X_t; Y_t, t) \leq \mathring{\mathcal{L}}(W_t; Y_t, t) + \beta\sqrt{t}\varepsilon_t^2/2$ . In this sense,  $X_t$  is an approximation to  $W_t$ . In fact, by the strong convexity of  $\mathring{\mathcal{L}}(X; Y_t, t)$  with respect to the  $\|\cdot\|_1$  norm, we have  $\beta\sqrt{t}\varepsilon_t^2/2 \geq \mathring{\mathcal{L}}(X_t; Y_t, t) - \mathring{\mathcal{L}}_* \geq (\beta\sqrt{t}/2)\|X_t - W_t\|_1^2$ . Therefore, we assert that  $\|X_t - W_t\|_1 \leq \varepsilon_t$ , and consequently  $\text{tr}((W_t - X_t)S_{t+1}) \leq \psi_{t+1}\|X_t - W_t\|_1 \leq \varepsilon_t\psi_{t+1}$ .

Next, Lemma 1 of [Orabona et al. \(2015\)](#) shows that

$$\sum_{t=1}^T \text{tr}(S_{t+1}(\Pi - W_t)) \leq f_T(\Pi) + \sum_{t=1}^T \left\{ \frac{\psi_{t+1}^2}{2\beta\sqrt{t}} + f_{t-1}(W_t) - f_t(W_t) \right\}. \quad (40)$$

Then adding the  $\text{tr}((W_t - X_t)S_{t+1})$  term to the left hand side of (40) yields

$$\begin{aligned} \sum_{t=1}^T \text{tr}(S_{t+1}(\Pi - X_t)) &\leq f_T(\Pi) + \sum_{t=1}^T \left\{ \frac{\psi_{t+1}^2}{2\beta\sqrt{t}} + \varepsilon_t\psi_{t+1} + (\sqrt{t-1} - \sqrt{t})g(W_t) - F(W_t) \right\} \\ &\leq \sqrt{T}g(\Pi) + TF(\Pi) + \sum_{t=1}^T \left\{ \frac{\psi_{t+1}^2}{2\beta\sqrt{t}} + \varepsilon_t\psi_{t+1} - F(W_t) \right\}. \end{aligned} \quad (41)$$

Note that  $|F(W_t) - F(X_t)| = \lambda|\|W_t\|_{1,1} - \|X_t\|_{1,1}| \leq \lambda\|W_t - X_t\|_{1,1} \leq \lambda\varepsilon_t$ , so adding the inequality  $0 \leq F(W_t) - F(X_t) + \lambda\varepsilon_t$  to (41) gives

$$\sum_{t=1}^T \text{tr}(S_{t+1}(\Pi - X_t)) + \sum_{t=1}^T F(X_t) - TF(\Pi) \leq \sqrt{T}g(\Pi) + \sum_{t=1}^T \left\{ \frac{\psi_{t+1}^2}{2\beta\sqrt{t}} + \varepsilon_t(\lambda + \psi_{t+1}) \right\}.$$

Finally,  $d_{\mathcal{K}}(\Pi) = 0$ , and  $d_{\mathcal{K}}(X_t) \leq \beta\sqrt{t}\varepsilon_t^2/2$  by Theorem 1(b), so the first part of the theorem is proved.

Now consider the final output  $\hat{X}_T = X_T$ . Define  $Z_T = \mathcal{P}_{\mathcal{K}}(X_T)$ ,  $S = T^{-1}\sum_{t=1}^T S_t$ ,  $\mathcal{L}(X) = T^{-1}\mathring{\mathcal{L}}(X; \alpha TS, T)$ , and  $\mathcal{L}_* = \min_{X \in \mathcal{X}} \mathcal{L}(X)$ . Then by Algorithm 3 and Theorem 1, we have  $\mathcal{L}(Z_T) \leq \mathcal{L}_* + \beta\varepsilon_T^2/(2\sqrt{T})$  and  $\|X_T - Z_T\|_F \leq \beta\sqrt{T}\varepsilon_T^2/2$ . Define  $\Delta = Z_T - \Pi$  and  $W = S - \Sigma$ . Similar to the proof of Corollary 2, if  $\lambda \geq \|W\|_{\infty}$ , then

$$\begin{aligned} (\delta_d/2)\|\Delta\|_F^2 &\leq -\text{tr}(\Sigma\Delta) = -\text{tr}(S\Delta) + \text{tr}(W\Delta) \\ &= \mathcal{L}(Z_T) - \mathcal{L}(\Pi) - \lambda(\|Z_T\|_1 - \|\Pi\|_1) + \text{tr}(W\Delta) - (\rho(Z_T) - \rho(\Pi))/\sqrt{T} \\ &\leq \beta\varepsilon_T^2/(2\sqrt{T}) + 2\lambda s\|\Delta\|_F - (\rho(Z_T) - \rho(\Pi))/\sqrt{T}. \end{aligned}$$

Due to the strong convexity of  $\rho(X)$ , we have  $\rho(Z_T) - \rho(\Pi) \geq \text{tr}(U\Delta) + (\beta/2)\|\Delta\|_1^2 \geq -\|U\|_F\|\Delta\|_F + (\beta/2)\|\Delta\|_F^2$ , where  $U = \nabla\rho(\Pi)$ . Since  $\Pi$  is sparse, the norm of  $\Pi$  can be computed on an  $s \times s$  submatrix. Therefore, using (39) again we get  $\|\nabla\rho(\Pi)\|_F = \|\Pi\|_r^{2-r} \cdot \|\Pi\|_{2r-2}^{r-1} \leq s^{2-4/\log(p)}\|\Pi\|_F = s^{2-4/\log(p)}\sqrt{d}$ . Further take  $\varepsilon_T = 1/\sqrt{T}$ , and then

$$(\delta_d + \beta/\sqrt{T})/2 \cdot \|\Delta\|_F^2 \leq \frac{\beta}{2T^{3/2}} + \left( 2\lambda s + \frac{\|U\|_F}{\sqrt{T}} \right) \|\Delta\|_F.$$

Solving the inequality and noting that  $\|X_T - Z_T\|_F \leq \beta\sqrt{T}\varepsilon_T^2/2 = \beta/(2\sqrt{T})$ , we get the claimed bound.

## References

- Bertsekas, D. P. (2011). Incremental proximal methods for large scale convex optimization. *Mathematical Programming*, 129(2):163.
- Boyd, S., Parikh, N., Chu, E., Peleato, B., and Eckstein, J. (2011). Distributed optimization and statistical learning via the alternating direction method of multipliers. *Foundations and Trends® in Machine learning*, 3(1):1–122.
- Chen, K. and Lei, J. (2015). Localized functional principal component analysis. *Journal of the American Statistical Association*, 110(511):1266–1275.
- Chen, Y. and Wainwright, M. J. (2015). Fast low-rank estimation by projected gradient descent: General statistical and algorithmic guarantees. *arXiv preprint arXiv:1509.03025*.
- d’Aspremont, A., Ghaoui, L. E., Jordan, M. I., and Lanckriet, G. R. (2005). A direct formulation for sparse pca using semidefinite programming. In *Advances in Neural Information Processing Systems 17*, pages 41–48.
- Friedman, J., Hastie, T., and Tibshirani, R. (2008). Sparse inverse covariance estimation with the graphical lasso. *Biostatistics*, 9(3):432–441.
- Fromer, M., Roussos, P., Sieberts, S. K., Johnson, J. S., Kavanagh, D. H., Perumal, T. M., Ruderfer, D. M., Oh, E. C., Topol, A., Shah, H. R., et al. (2016). Gene expression elucidates functional impact of polygenic risk for schizophrenia. *Nature Neuroscience*, 19(11):1442.
- Gajjar, S., Kulahci, M., and Palazoglu, A. (2018). Real-time fault detection and diagnosis using sparse principal component analysis. *Journal of Process Control*, 67:112–128.
- Grbovic, M., Li, W., Xu, P., Usadi, A. K., Song, L., and Vucetic, S. (2012). Decentralized fault detection and diagnosis via sparse pca based decomposition and maximum entropy decision fusion. *Journal of Process Control*, 22(4):738–750.
- Hotelling, H. (1933). Analysis of a complex of statistical variables into principal components. *Journal of Educational Psychology*, 24(6):417.
- Johnstone, I. M. and Lu, A. Y. (2009). On consistency and sparsity for principal components analysis in high dimensions. *Journal of the American Statistical Association*, 104(486):682–693.

- Jolliffe, I. T., Trendafilov, N. T., and Uddin, M. (2003). A modified principal component technique based on the lasso. *Journal of Computational and Graphical Statistics*, 12(3):531–547.
- Journée, M., Nesterov, Y., Richtárik, P., and Sepulchre, R. (2010). Generalized power method for sparse principal component analysis. *Journal of Machine Learning Research*, 11(Feb):517–553.
- Jung, S. and Marron, J. S. (2009). Pca consistency in high dimension, low sample size context. *The Annals of Statistics*, 37(6B):4104–4130.
- Kakade, S. M., Shalev-Shwartz, S., and Tewari, A. (2012). Regularization techniques for learning with matrices. *Journal of Machine Learning Research*, 13(Jun):1865–1890.
- Kundu, A., Bach, F., and Bhattacharya, C. (2018). Convex optimization over intersection of simple sets: improved convergence rate guarantees via an exact penalty approach. In *Proceedings of the Twenty-First International Conference on Artificial Intelligence and Statistics*, pages 958–967.
- Lee, S., Epstein, M. P., Duncan, R., and Lin, X. (2012). Sparse principal component analysis for identifying ancestry-informative markers in genome-wide association studies. *Genetic Epidemiology*, 36(4):293–302.
- Lei, J. and Vu, V. Q. (2015). Sparsistency and agnostic inference in sparse pca. *The Annals of Statistics*, 43(1):299–322.
- Li, C. J., Wang, M., Liu, H., and Zhang, T. (2018). Near-optimal stochastic approximation for online principal component estimation. *Mathematical Programming*, 167(1):75–97.
- Ma, Z. (2013). Sparse principal component analysis and iterative thresholding. *The Annals of Statistics*, 41(2):772–801.
- Mahdavi, M., Yang, T., Jin, R., Zhu, S., and Yi, J. (2012). Stochastic gradient descent with only one projection. In *Advances in Neural Information Processing Systems 25*, pages 494–502.
- Marinov, T. V., Mianjy, P., and Arora, R. (2018). Streaming principal component analysis in noisy settings. In *Proceedings of the 35th International Conference on Machine Learning*, pages 3410–3419.
- Oja, E. and Karhunen, J. (1985). On stochastic approximation of the eigenvectors and eigenvalues of the expectation of a random matrix. *Journal of Mathematical Analysis and Applications*, 106(1):69–84.
- Orabona, F., Crammer, K., and Cesa-Bianchi, N. (2015). A generalized online mirror descent with applications to classification and regression. *Machine Learning*, 99(3):411–435.

- Pearson, K. (1901). Liii. on lines and planes of closest fit to systems of points in space. *The London, Edinburgh, and Dublin Philosophical Magazine and Journal of Science*, 2(11):559–572.
- Ryu, E. K. and Yin, W. (2017). Proximal-proximal-gradient method. *arXiv preprint arXiv:1708.06908*.
- She, Y. (2017). Selective factor extraction in high dimensions. *Biometrika*, 104(1):97–110.
- Shen, H. and Huang, J. Z. (2008). Sparse principal component analysis via regularized low rank matrix approximation. *Journal of Multivariate Analysis*, 99(6):1015–1034.
- Stuart, J. M., Segal, E., Koller, D., and Kim, S. K. (2003). A gene-coexpression network for global discovery of conserved genetic modules. *Science*, 302(5643):249–255.
- Tan, K. M., Wang, Z., Liu, H., and Zhang, T. (2018). Sparse generalized eigenvalue problem: optimal statistical rates via truncated rayleigh flow. *Journal of the Royal Statistical Society: Series B (Statistical Methodology)*, 80(5):1057–1086.
- Tibshirani, R. J. (2014). Adaptive piecewise polynomial estimation via trend filtering. *The Annals of Statistics*, 42(1):285–323.
- Vu, V. Q., Cho, J., Lei, J., and Rohe, K. (2013). Fantope projection and selection: A near-optimal convex relaxation of sparse pca. In *Advances in Neural Information Processing Systems 26*, pages 2670–2678.
- Vu, V. Q. and Lei, J. (2013). Minimax sparse principal subspace estimation in high dimensions. *The Annals of Statistics*, 41(6):2905–2947.
- Wang, C. and Lu, Y. M. (2016). Online learning for sparse pca in high dimensions: Exact dynamics and phase transitions. In *2016 IEEE Information Theory Workshop (ITW)*, pages 186–190. IEEE.
- Wang, Z., Lu, H., and Liu, H. (2014). Nonconvex statistical optimization: minimax-optimal sparse pca in polynomial time. *arXiv preprint arXiv:1408.5352*.
- Warmuth, M. K. and Kuzmin, D. (2008). Randomized online pca algorithms with regret bounds that are logarithmic in the dimension. *Journal of Machine Learning Research*, 9(Oct):2287–2320.
- Witten, D. M., Tibshirani, R., and Hastie, T. (2009). A penalized matrix decomposition, with applications to sparse principal components and canonical correlation analysis. *Biostatistics*, 10(3):515–534.
- Yang, T., Lin, Q., and Zhang, L. (2017). A richer theory of convex constrained optimization with reduced projections and improved rates. In *Proceedings of the 34th International Conference on Machine Learning*, pages 3901–3910.

- Yang, W. and Xu, H. (2015). Streaming sparse principal component analysis. In *Proceedings of the 32nd International Conference on Machine Learning*, pages 494–503.
- Zhang, B. and Horvath, S. (2005). A general framework for weighted gene co-expression network analysis. *Statistical Applications in Genetics and Molecular Biology*, 4(1).
- Zhang, Y. and Ghaoui, L. E. (2011). Large-scale sparse principal component analysis with application to text data. In *Advances in Neural Information Processing Systems 24*, pages 532–539.
- Zhu, L., Lei, J., Devlin, B., and Roeder, K. (2017). Testing high-dimensional covariance matrices, with application to detecting schizophrenia risk genes. *The Annals of Applied Statistics*, 11(3):1810.
- Zou, H., Hastie, T., and Tibshirani, R. (2006). Sparse principal component analysis. *Journal of Computational and Graphical Statistics*, 15(2):265–286.
- Zou, H. and Xue, L. (2018). A selective overview of sparse principal component analysis. *Proceedings of the IEEE*, 106(8):1311–1320.